

AD-A077 041 GEORGIA INST OF TECH ATLANTA ENGINEERING EXPERIMENT --ETC F/8 6/16
IN-VIVO TECHNIQUES FOR MEASURING ELECTRICAL PROPERTIES OF TISSU--ETC(U)
JUL 79 E C BURDETTE , R L SEAMAN , J SEALS DAMD17-78-C-8044
UNCLASSIFIED GIT/EES-A-2171-1 NL

1 OF 1
AD
A077041



AD A 077041

ANNUAL TECHNICAL REPORT NO. 1
PROJECT A-2171

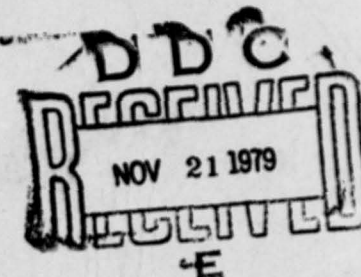
AD 12

LEVEL 12

**IN-VIVO TECHNIQUES FOR MEASURING
ELECTRICAL PROPERTIES OF TISSUES**

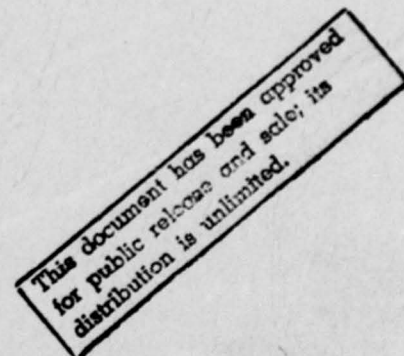
By

E. C. Burdette, R. L. Seaman, J. Seals, and F. L. Cain



Prepared for

U.S. ARMY MEDICAL RESEARCH AND
DEVELOPMENT COMMAND
FORT DETRICK
FREDERICK, MARYLAND 21701
CONTRACT NO. DAMD17-78-C-8044



Submitted by

BIOMEDICAL RESEARCH GROUP
ELECTRONICS TECHNOLOGY LABORATORY

DDC FILE COPY

July 1979

GEORGIA INSTITUTE OF TECHNOLOGY

Engineering Experiment Station
Atlanta, Georgia 30332



1979



79 11 20 184

UNCLASSIFIED

SECURITY CLASSIFICATION OF THIS PAGE (When Data Entered)

REPORT DOCUMENTATION PAGE		READ INSTRUCTIONS BEFORE COMPLETING FORM
1. REPORT NUMBER	2. GOVT ACCESSION NO.	3. RECIPIENT'S CATALOG NUMBER
4. TITLE (and Subtitle) "In-vivo Techniques for Measuring Electrical Properties of Tissues"		5. TYPE OF REPORT & PERIOD COVERED Annual Technical Report No. 1 1 July 78 - 30 June 79
7. AUTHOR(s) E.C. Burdette, and, F.L. Cain R.L. Seaman J. Seals		6. PERFORMING ORG. REPORT NUMBER A-2171-1 8. CONTRACT OR GRANT NUMBER(s) DAMD17-78-C-8044
9. PERFORMING ORGANIZATION NAME AND ADDRESS Engineering Experiment Station Georgia Institute of Technology Atlanta, Georgia 30332		10. PROGRAM ELEMENT, PROJECT, TASK AREA & WORK UNIT NUMBERS 12 8P
11. CONTROLLING OFFICE NAME AND ADDRESS		12. REPORT DATE July 1979
14. MONITORING AGENCY NAME & ADDRESS (if different from Controlling Office) U.S. Army Medical Research & Development Command Fort Detrick Frederick, Maryland 21701		13. NUMBER OF PAGES 71 + vi
		15. SECURITY CLASS. (of this report) Unclassified
		15a. DECLASSIFICATION/DOWNGRADING SCHEDULE
16. DISTRIBUTION STATEMENT (of this Report) Approved for Public Release; Distribution Unlimited		
17. DISTRIBUTION STATEMENT (of the abstract entered in Block 20, if different from Report) Approved for Public Release; Distribution Unlimited		
18. SUPPLEMENTARY NOTES		
19. KEY WORDS (Continue on reverse side if necessary and identify by block number) <u>In-vivo</u> probe Electromagnetic energy Dielectric properties Monopole antenna <u>In-situ</u> tissues		
20. ABSTRACT (Continue on reverse side if necessary and identify by block number) The overall objectives of this research investigation are to further develop and extend the capabilities of the recently-developed <u>in-vivo</u> probe measurement technique and to use this technique to study the possible effects of induced physiological changes on tissue dielectric properties. During the first year of this two-year program, the research efforts conducted included (1) development of techniques for improved probe positioning flexibility, (2) implementation of methods to account for systemic microwave measurement errors, (3) development of techniques for rapid data collection, (4) evaluation of effects		

DD FORM 1473

1 JAN 73

EDITION OF 1 NOV 65 IS OBSOLETE

UNCLASSIFIED

SECURITY CLASSIFICATION OF THIS PAGE (When Data Entered)

UNCLASSIFIED

SECURITY CLASSIFICATION OF THIS PAGE(When Data Entered)

of surface fluid accumulation around the probe, (5) establishment of a probe diameter/sample volume relationship, (6) probe dielectric measurements of living and non-living canine brain, and (7) preliminary measurements of canine brain dielectric properties as a function of induced physiological changes including non-noxious auditory stimuli. Little or no effect by the acoustic stimuli on the dielectric properties was observed. However, the lack of positive results from experiments involving acoustic stimuli could have been due to the preliminary nature of these experiments. Data for measurements made on live brain in four dogs indicate a general decrease in dielectric constant and conductivity as a function of depth below the surface of the brain, which could be due to differences in blood flow, metabolism, or a combination of both. Significant differences in the dielectric properties of living and non-living canine brain were observed when measured as a function of time after death.

Accession For	
NTIS GRA&I	<input checked="checked" type="checkbox"/>
DDC TAB	<input type="checkbox"/>
Unannounced	<input type="checkbox"/>
Justification	
By _____	
Distribution/	
Availability	
Dist	Avail and/or special

UNCLASSIFIED

SECURITY CLASSIFICATION OF THIS PAGE(When Data Entered)

ANNUAL TECHNICAL REPORT NO. 1

PROJECT A-2171

IN-VIVO TECHNIQUES FOR MEASURING ELECTRICAL PROPERTIES OF TISSUES

By

E.C. Burdette, R.L. Seaman, J. Seals, and F.L. Cain

JULY 1979

Prepared for

U.S. Army
Medical Research and Development Command
Fort Detrick
Frederick, Maryland 21701

Prepared by

Biomedical Research Group
Electronics Technology Laboratory
Engineering Experiment Station
Georgia Institute of Technology
Atlanta, Georgia 30332

SUMMARY

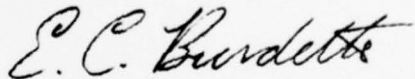
↘ The overall objectives of this research investigation are to further develop and extend the capabilities of the recently-developed in-vivo probe measurement technique and to use this technique to study the possible effects of induced physiological changes on tissue dielectric properties. During the first year of this two-year program, the research efforts conducted included (1) development of techniques for improved probe positioning flexibility, (2) implementation of methods to account for systemic microwave measurement errors, (3) development of techniques for rapid data collection, (4) evaluation of effects of surface fluid accumulation around the probe, (5) establishment of a probe diameter/sample volume relationship, (6) probe dielectric measurements of living and non-living canine brain, and (7) preliminary measurements of canine brain dielectric properties as a function of induced physiological changes including non-noxious auditory stimuli. Little or no effect by the acoustic stimuli on the dielectric properties was observed. ↗ However, the lack of positive results from experiments involving acoustic stimuli could have been due to the preliminary nature of these experiments. Data from measurements made on live brain in four dogs indicate a general decrease in dielectric constant and conductivity as a function of depth below the surface of the brain, which could be due to differences in blood flow, metabolism, or a combination of both. Significant differences in the dielectric properties of living and non-living canine brain were observed when measured as a function of time after death.

FOREWORD

The research on the first year of this two-year program was carried out by personnel of the Biomedical Research Group of the Electronics Technology Laboratory of the Engineering Experiment Station at the Georgia Institute of Technology, Atlanta, Georgia 30332. Mr. F.L. Cain served as the Principal Investigator and Mr. E.C. Burdette served as the Associate Principal Investigator. The program, which is sponsored by the U.S. Army Research and Development Command, Fort Detrick, Frederick, Maryland 21701, under Contract NO. DAMD17-78-C-8044, is designated by Georgia Tech as Project A-2171.

This Annual Technical Report covers the work which was performed from 1 July 1978 through 30 June 1979. This work was made possible through the combined efforts of many people at the Walter Reed Army Institute of Research (WRAIR), at the Emory University School of Medicine, and at the Georgia Institute of Technology. The authors would especially like to thank Dr. L.E. Larsen and Mr. J.H. Jacobi at WRAIR and Dr. V.P. Popovic at the Emory University School of Medicine, all of whom contributed significantly to the first year's success of this research program.

Respectfully submitted,



E.C. Burdette
Associate Principal Investigator

Approved:



Fred L. Cain
Principal Investigator
Associate Director,
Electronics Technology Laboratory

TABLE OF CONTENTS

<u>Section</u>	<u>Page</u>
I. INTRODUCTION.	1
A. Research Objectives	2
B. Summary of First Year Efforts	3
II. PROBE DESIGN AND DEVELOPMENT.	7
A. Theoretical Basis	7
B. Recent Developmental Efforts.	9
C. Frequency Range, Sample Volume, and Fabrication Considerations.	15
III. MEASUREMENT SYSTEM DEVELOPMENT.	22
A. Network Analyzer Based Instrumentation.	22
B. Microwave Measurement Error Correction and Calibration	33
C. Evaluation of System Performance.	35
IV. EXPERIMENTAL INVESTIGATIONS	41
A. Physiological Instrumentation and Surgical Equipment	41
B. Laboratory Procedures	44
C. Measurement Results	48
V. CONCLUSIONS AND RECOMMENDATIONS	65
A. Conclusions from Results.	65
B. Recommended Second Year Tasks	68
C. Recommended Future Efforts.	69
VI. REFERENCES.	70

LIST OF FIGURES

Figure		Page
1.	Insertion loss of Gore-Tex cable.	12
2.	Phase of measured reflection coefficient for muscle under two conditions of fluid accumulation on tissue prior to measurement.	14
3.	Phase of measured reflection coefficient for muscle under conditions where fluid accumulation was controlled. Data presented are four repeated measurements.	16
4.	Two configurations of the monopole dielectric measurement probe	18
5.	Minimum sample volume required for accurate dielectric property determination as a function of probe diameter for the infinitesimal probe. This relationship is valid only for medium- and high-loss samples	21
6.	Block diagram of manually-operated <u>in-vivo</u> probe measurement system used in the initial experiments.	24
7.	Block diagram of the present semi-automated data acquisition/data processing <u>in-vivo</u> probe measurement system.	25
8.	Wiring diagram of Commodore PET computer to analogic combination multiplexer/analog to digital converter	28
9.	Flow chart of algorithm for single frequency measurements	29
10.	Flow chart of algorithm for multiple frequency measurements	31
11.	Sample printout of dielectric property data measured for deionized water using single frequency program in the automatic mode.	32
12.	Error models used for test set/connection errors.	34
13.	(a) Amplitude and (b) Phase of corrected and uncorrected short circuit termination reflection coefficient data	37
14.	Relative dielectric constant of (a) water and (b) methanol measured at a temperature of 20°C with and without systemic error correction.	39
15.	Loss tangent of (a) water and (b) methanol measured at a temperature of 20°C with and without systemic error correction.	40
16.	View of experimental animal positioned in stereotaxic apparatus for recording dielectric and physiological data	42
17.	Probe in position for measurements of <u>in-vivo</u> dielectric properties of pial surface.	47
18.	Measured dielectric properties of dura before and during bag breathing. The shaded area denotes bag breathing. Time is the time from the start of measurements. Brain temperature range: 35.3 to 35.5°C.	50

LIST OF FIGURES (continued)

<u>Figure</u>		<u>Page</u>
19.	Measured dielectric properties of deep canine brain (white matter) as a function of time after death resulting from pentobarbital overdose injection. Brain temperature range: 36.5 to 38.5°C.	52
20.	Measured dielectric properties of shallow canine brain (gray matter) as a function of time after death resulting from pentobarbital overdose injection. Brain temperature range: 34.0 to 37.5°C.	53
21.	Measured dielectric properties of surface of brain as a function of time after death resulting from CaCl_2 injection. Brain temperature range: 35.5 to 36.0°C.	55
22.	Results of dural measurements in acoustic stimulation experiment: solid circles are for 300 Hz; open circles, 5 kHz. Refer to text for further details	58
23.	Results of pial measurements in acoustic stimulation experiment. Solid circles are for 200 Hz; open circles, 5 kHz. Refer to text for further details	59
24.	Summary of <u>in-vivo</u> brain data from four animals. Column height is the mean value. The bars indicate plus or minus one standard deviation.	61

SECTION I

INTRODUCTION

The research described in this Annual Report is the result of efforts performed during the first year of this two-year research program. The overall objectives of this research investigation are to further develop and extend the capabilities of the recently-developed in-vivo probe dielectric property measurement technique [1-3] and to use this technique to study induced physiological changes in organs or organ systems which affect various tissue components, and hence, the tissue dielectric properties. Because the dielectric properties of a living system determine the coupling and absorption of non-ionizing electromagnetic (EM) energy by that system, knowledge of the in-situ properties of the living tissue is essential both to effectively employ EM radiation in biomedical applications and to adequately determine safe levels for personnel exposure to EM radiation. Both in the determination of EM radiation hazards with respect to personnel and in beneficial applications of EM energy, the EM field interaction with the tissue is primarily dependent upon the local geometry and the dielectric properties of the tissue. The in-vivo dielectric properties would necessarily reflect physiological characteristics and conditions, that in turn affect the absorbed EM power and its spatial distribution, which cannot be obtained through in-vitro dielectric measurements.

Several methods are available for measuring the dielectric properties of biological tissues [4]. However, the majority of these techniques require tissue excision, which makes the measurement of in-vivo dielectric properties of the tissue impossible [5]. Further, the correlation of possible changes in tissue dielectric characteristics as a function of physiological changes cannot be determined from in-vitro measurements. Also, most conventional measurement techniques require careful preparation of the excised tissue sample in order to conform to the dimensions of a special sample holder. Because of the sensitivity of these measurement techniques to variations in sample preparation and because of the difficulties in preparing precise tissue samples,

adequate tissue sample preparation is often a major source of measurement error. Another shortcoming of most conventional dielectric measurement techniques is their limited frequency range of operation, which makes it necessary to implement several different measurement systems in order to obtain data over an appreciable frequency range.

The problems of conventional dielectric property measurement techniques have been overcome by the recent development of an in-vivo probe measurement technique under Army support [2-3]. The measurement concept used to develop this new technique is based on the use of an antenna modeling theorem and has been automated/extended by the application of more precise, microprocessor-controlled, microwave measurement instrumentation. The theorem relates the change in free-space terminal impedance of a monopole antenna when inserted into a material to the dielectric properties of that material [6]. A short monopole antenna, suitable for insertion into living tissue, is used as the in-vivo probe. Measurement equipment used with the probe includes a signal source, reflectometer, Hewlett-Packard network analyzer, and a semi-automated data-acquisition/data-processing system. These VHF/microwave measurement equipment and data processing system permit accurate determination of the impedance characteristics of the probe, and consequently, of desired tissue electrical characteristics.

A. Research Objectives

The objectives of this two-year research program are to further develop and extend the in-vivo probe measurement technique for determining tissue dielectric characteristics, to use this technique to study possible changes in dielectric properties resulting from physiological changes, and to investigate differences between tissue dielectric properties determined in-vivo versus those determined in-vitro. Specific areas of investigation include (1) extending the capabilities of the recently developed in-vivo probe measurement techniques [1-3], (2) elucidating differences between the in-situ dielectric properties of living tissue and dielectric properties of tissue determined in-vitro, and (3) correlating changes in the in-vivo dielectric properties of brain with physiological changes (regional

cerebral blood flow) due to hypercapnic and anoxic conditions and to non-noxious sensory stimuli. A long term objective is the extension of the probe technique as a method for quantitative determination of local blood flow changes in brain and possibly kidney without the need for radioactive tracers and tissue excision.

B. Summary of First Year Efforts

The investigations described in this report were performed during the first year of this two-year research contract. The tasks performed during these first-year investigations include (1) the development of techniques for increased flexibility in probe positioning, (2) implementation of methods to account for measurement errors associated with the microwave measurement instrumentation, (3) the development of techniques for rapid data collection and processing, (4) evaluation of the effects of surface fluid accumulation around the probe, (5) fabrication of different sized probes for measurements of tissue samples of varied volumes, (6) probe dielectric measurements of living and non-living brain, and (7) preliminary measurements of canine brain dielectric properties as a function of induced physiological changes. These efforts are briefly summarized below.

Under previous research efforts [2,3], it was determined that probe positioning was a critical factor in the performance of accurate in-vivo dielectric measurements. Further, it was determined that positioning of the probe needed to be made more compatible with measurement conditions associated with animals larger than mice or rats, which were positioned beneath a fixed measurement probe. Several alternative methods involving the use of semi-rigid or flexible coaxial cable attached to the in-vivo measurement probe were evaluated. The technical requirements of a suitable cable for use with the probe were the following: a length adequate to allow the probe to be positioned on a large experimental animal and still permit convenient location of the network analyzer, adequate cable flexibility for ease in repositioning, introduction of minimal phase variations due to cable movement, low attenuation and VSWR, and the ability to withstand sterilization.

Following an examination of cables from nearly a dozen manufacturers, it was determined that the most suitable cable for use with the in-vivo probe measurement system was the Gore-Tex® flexible cable. This cable is doubly shielded with an outer conductor of two silver-plated copper shields, contains an expanded polytetrafluoroethylene (PTFE) dielectric, and has a stranded silver-plated copper center conductor. The electrical specifications of the cable are within the requirements of the probe measurement system, with the most critical parameter being phase variation with cable movement. Published data for Gore-Tex® flexible cable specify a maximum phase variation of two degrees at 10 GHz when the cable is bent around a three-inch mandrel. Also, Gore-Tex® cable may be gas sterilized without any deterioration in performance. A three-foot length cable, including connectors, was tested and found to perform adequately over the frequency range examined (2-4 GHz).

An investigation of the accuracy of the results obtained from measurements of standard dielectric materials indicated a need to evaluate the residual systemic errors associated with the network analyzer measurement system. An existing model [3] for reduction of microwave measurement errors (directivity, source match, frequency tracking) associated with the network analyzer, reflectometer, and interconnecting cables was further developed to include multiple-load data in the determination of the directivity error. Also, the systemic error correction model was incorporated in a microprocessor-based data acquisition/data processing system. The error correction is performed through measurements of terminations (short circuits, open circuits, and a sliding matched load) for which the reflection coefficients are known. From these measurements, the error terms are computed using the error correction model and the measured tissue sample data are corrected to account for the systemic measurement errors.

The semi-automated microprocessor-based data acquisition system developed previously [3] was modified and upgraded during this first year of the program. Specifically, a digital frequency locking capability was added to the system, an external keyboard/printer was interfaced, and the entire computer algorithm was rewritten both to increase the flexibility and data processing capability of the system

and to accommodate the additional system hardware. The present semi-automated data acquisition/data processing system utilizes a Commodore PET 2001-8 computer as the central element. Other hardware items include the printer and printer interface, an IEEE Standard 488-1975 compatible bus which interfaces to a Hewlett-Packard digital frequency counter and sweep frequency generator, and a parallel interface to a 12-bit analog-to-digital converter/multiplexer. This data acquisition system permits both rapid, accurate data collection and correction of the inherent directivity, source match, and frequency tracking systemic measurement errors. The system automatically collects measured reflection coefficient data from the probe, processes these data, and outputs corrected dielectric property information. Measurements may be made either over swept frequency bands between 0.1 GHz and 10 GHz or as a function of time at a single frequency.

Effort was also directed toward the evaluation of the effects of fluid accumulation in the vicinity of the probe. Excessive fluid accumulation affects both the accuracy of the dielectric measurements and the repeatability of the measurements. It was determined that fluid accumulation around the probe did not appreciably affect the results of dielectric measurements of high-loss tissues. However, significant effects of fluid accumulation were observed in the results of measurements on relatively low-loss tissues. After investigating several methods of preventing the fluid accumulation, it was determined that the following simple approach yielded the most accurate and consistent results. First, the probe tip should be thoroughly cleaned between each sequence of measurements. This cleaning prevents any residue of fluids from drying on the tip of the probe and acting as an insulating layer between the probe and tissue during subsequent measurements. Second, adequate probe contact with the measurement area is essential to obtaining accurate results. Excessive contact pressure is not required, but complete, uniform contact with the tissue is necessary. Finally, the best way to prevent fluid buildup around the outer conductor of the probe is simply to use cotton-tipped swabs and small 2-inch by 2-inch absorbent gauze pads. These simple procedures

prevent fluid accumulation and seepage into the probe contact region, and the use of a clean probe ensures good electrical contact.

Attention has also been given to probe fabrication techniques and factors influencing measured sample volume and useful frequency range. In addition to sources of measurement error previously mentioned, errors in measurement accuracy have resulted from factors such as imperfect attachment of probe connectors and variations in the manufactured quality of materials from which the probes are fabricated. These factors also affect the useful frequency range of the fabricated probes. During the first year of this program, additional techniques for ensuring good probe fabrication were implemented which are detailed in Section II. It was also learned from studies of the influence of probe diameter on measured sample volume of lossy tissue that the thickness of the sample must be between one and two probe diameters to ensure measurement accuracy and that low-loss samples must have an even greater thickness.

Finally, preliminary in-situ measurements of living and non-living brain and of in-vivo dielectric properties of brain under conditions of induced physiological change were performed as a part of the first-year efforts. All measurements were performed at a frequency of 2450 MHz using a probe having a diameter comparable to that of a No. 16 hypodermic needle. In-situ dielectric measurements of both living and non-living canine brain were performed on the dura, on the pia, and in gray and white matter. In the case of dural measurements, one case of normal and anoxic conditions was examined. Pial dielectric measurements were conducted in one experiment in which a non-noxious auditory stimulus was applied, and measurements of dielectric properties as a function of time after death were performed both in brain and on the pial surface in separate experiments. The results of these experimental studies are described in Section IV.

SECTION II

PROBE DESIGN AND DEVELOPMENT

In this section, the design and development of the dielectric measurement probe itself is discussed with special emphasis on those factors relating to the experimental investigations conducted during the first year of this research program. Specifically, design parameters and influencing measurement factors including (1) the development of an increased probe positioning flexibility, (2) evaluation of probe contact pressure and the effects of fluid accumulation around the probe, and (3) frequency range/probe diameter/sample volume relationships are addressed. Additionally, considerations in the probe fabrication process are presented.

A. Theoretical Basis

Before discussing physical probe design and developmental efforts, it is appropriate to mention the theoretical basis underlying the in-vivo dielectric measurement probe. Detailed analyses of theoretical aspects of the probe have been previously presented [1-3], but only recently were the various theoretical considerations presented in a single report [7]. Because the details of these analyses have been previously reported, only a brief synopsis of the theory is given here.

The theoretical basis of the in-vivo measurement probe stems from the application of an antenna modeling theorem to the characterization of unknown dielectric media [3,6,8]. Simply stated, the antenna modeling theorem equates the terminal impedance of an antenna operating at frequency ω in a dielectric material to its terminal impedance in free space at frequency n , where n is the complex index of refraction of the dielectric material. In a non-magnetic material ($\mu=\mu_0$), the theorem is expressed mathematically as

$$\frac{Z(\omega, \epsilon^*)}{\eta} = \frac{Z(n\omega, \epsilon_0)}{\eta_0}, \quad (1)$$

where $\omega = 2\pi f$	= angular frequency (radians),
$\eta = \sqrt{\mu_0 / \epsilon^*}$	= the complex intrinsic impedance of the dielectric medium,
$\epsilon^* = \epsilon' - j\epsilon''$	= the complex permittivity of the dielectric medium,
$\eta_0 = \sqrt{\mu_0 / \epsilon_0}$	= the intrinsic impedance of free space,
ϵ_0	= the permittivity of free space, and
$n = \sqrt{\epsilon^* / \epsilon_0}$	= the complex index of refraction of the dielectric medium relative to that of air.

This theorem is applicable for any probe provided an analytical expression for the terminal impedance of the antenna is known both in free space and in the dielectric medium under study. The theorem as stated in Equation (1) assumes that the medium surrounding the antenna is infinite in extent, or conversely, the theorem is valid provided the probe's radiation field is contained completely within the medium.

For probe antennas one-tenth wavelength or less in length, the terminal impedance is given by

$$Z(\omega, \epsilon_0) = A\omega^2 + \frac{1}{jC\omega}, \quad (2)$$

where A and C are constants determined by the physical dimensions of the antenna [9]. From a knowledge of the above constants and the complex terminal impedance $Z(\omega, \epsilon^*)$ of the probe antenna in a dielectric material, the complex permittivity, and thus the relative dielectric constant, conductivity, and loss tangent values can be obtained from the theorem of Equation (1) by substitution.

For very short (or infinitesimal) monopole probes whose center conductor approaches zero length, the probe impedance in free space is totally reactive. In this case, the probe is essentially an open circuit transmission line having only a fringing field. Thus, the minimum sample volume necessary to obtain accurate measurement results is primarily dependent upon the distance between the tightly-coupled center and outer conductors of the probe. The free-space impedance of the open-circuited probe is simply

$$Z(\omega, \epsilon_0) = \frac{1}{jC\omega} , \quad (3)$$

where C is as indicated in Equation (2). Once again, the values of the dielectric properties are determined by substitution into the antenna modeling theorem.

B. Recent Developmental Efforts

The emphasis in development of the probe itself during the first year of this program has been placed on making the probe better suited for performing in-vivo dielectric measurements under various physiological conditions with minimum perturbation of those conditions. This development has included (1) an increased flexibility in probe positioning through the use of a special low-loss flexible cable, (2) an evaluation of the effects of fluid accumulation around the probe during an experimental measurement procedure, and (3) a study of the interrelationship of probe diameter, sample volume, and frequency range.

1. Flexible Cable Evaluation

Previously, in-vivo measurements were primarily performed under conditions where a small experimental animal (mouse or rat) was positioned beneath a fixed measurement probe [2,3]. A limited number of measurements involving larger animals were also performed [2], and for these cases, a standard RG-9B/U coaxial cable with N-type connectors and adapters to permit connection both to the probe and to the measurement instrumentation was used. Although increased probe flexibility was attained, the cable introduced highly position-dependent phase measurement errors, relatively high attenuation, and significant mismatches due to the VSWR of multiple connector/adaptor interfaces. The variability of measured data was quite large and it was evident that a more accurate and repeatable means of obtaining flexibility in probe positioning was required. To make the positioning of the in-vivo measurement probe more compatible with measurement conditions associated with larger experimental animal subjects, such as dogs, several alternate methods involving the use of semi-rigid or flexible coaxial

cable were evaluated. The technical requirements of a suitable cable were first identified, followed by a search for a commercially-available product that would satisfy those requirements. Specifically, the technical requirements established for a flexible (or semi-rigid) cable suitable for large animal in-vivo probe dielectric measurements included (1) a length adequate for suitable positioning of the probe and convenient location of the network analyzer, (2) high flexibility for ease in repositioning, (3) introduction of minimal phase error, (4) low attenuation and VSWR, and (5) ability to withstand sterilization without degradation of performance.

With these technical requirements in mind, a review of cable specifications published in manufacturers' catalogs was conducted. This review encompassed products manufactured by each of the following companies:

- Adams-Russel Co., Inc. (Amesbury, MA)
- American Microwave Cable (Waltham, MA)
- Andrew Corporation (Orland Park, IL)
- Astrolab, Inc. (Linden, NJ)
- Cablewave Systems, Inc. (North Haven, CT)
- Micro-Coax Cable (Collegeville, PA)
- Precision Tube, Co. (North Wales, PA)
- Prodelin Semi-Flexible Cables (Hightstown, NJ)
- Times Wire and Cable Co. (Wallingford, CT)
- W.L. Gore and Associates (Newark, DE).

When information from manufacturers' published specifications was compared with the technical requirements that the cable must meet, cables from three manufacturers appeared potentially satisfactory. These manufacturers were Adams-Russell Co., Inc.; Astrolab, Inc.; and W.L. Gore and Associates. Contact was made with each of these three companies to obtain further detailed information on characteristics such as phase stability as a function of flexure and the ability of the cable to withstand sterilization.

Adams-Russell, Inc., manufactured a cable known as FN Series Flexcable which exhibited adequate phase stability. However, additionally requested technical information was never received, and the verbal quote for a three-foot length of cable with a SMA connector on

one end and an APC-7 connector on the other end was quite high.

Additional technical information requested from Astrolab, Inc. on their Series 32000 cable was requested and received. These data revealed that phase variations from 8.4 degrees (at 2 GHz) to 40.9 degrees (at 10 GHz) occurred when the cable was wrapped around a 3-inch mandrel. Further, the data showed that these phase variations were retained by the cable when it was straightened and remeasured. This performance did not meet the requirements for use with the in-vivo probe measurement system because of the sensitivity of the computed dielectric constant to variations in the phase of the measured reflection coefficient.

A 3-foot length of Gore-Tex® cable manufactured by W.L. Gore and Associates has a specified phase variation of 2 degrees or less at a frequency of 10 GHz when wrapped around a 3-inch mandrel. The maximum phase variation as a function of temperature at 5.5 GHz is 10 degrees or less when the temperature is varied from -100°F to +250°F. The quoted cost for a 3-foot length of flexible cable with SMA connectors and an SMA-to-APC adapter was reasonable. This cable also met all other electrical requirements. The maximum specified VSWR at 18 GHz is 1.25:1, and the attenuation expressed in terms of insertion loss is shown in Figure 1. The Gore-Tex® flexible cable, having a capacitance of 26 pf/ft, is doubly shielded by two silver-plated copper shields: one is a copper foil 0.002-inch thick and the other is a conventional braid of AWG28 copper wire. Expanded polytetrafluoroethylene (PTFE) with a 70 percent air content comprises the dielectric, and the center conductor is 19-strand, AWG16, silver-plated copper wire. The combination of copper foil/copper braid outer conductor and stranded center conductor makes the cable quite flexible and well-suited for use with the in-vivo measurement probe.

Based on the information obtained from the catalogs and the manufacturers' representatives, the Gore-Tex® flexible cable was selected. The cable from Adams-Russell, Inc., appeared too expensive, and the Astrolab Series 32000 cable has an excessive phase variation both with flexure and with frequency for application in the probe

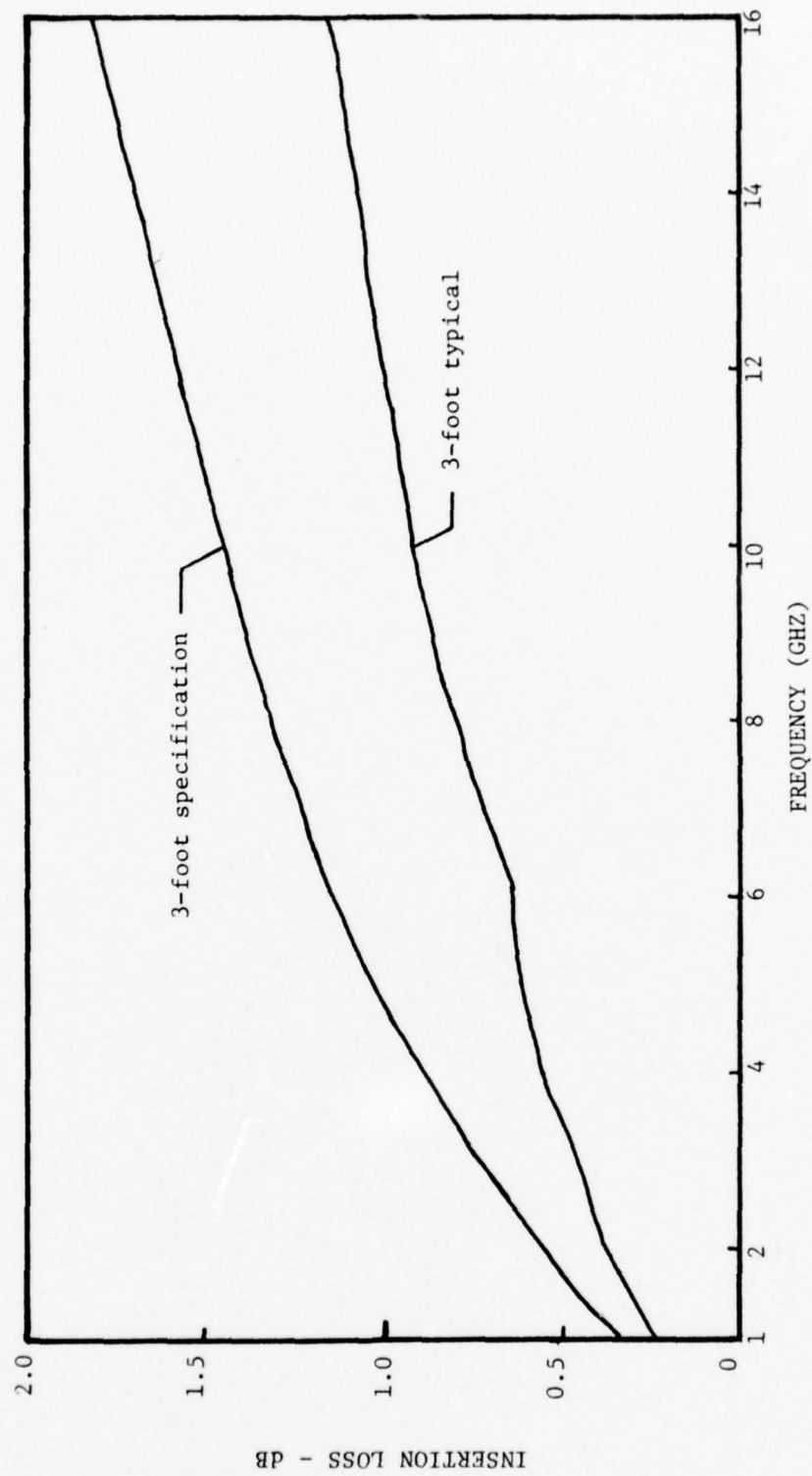


Figure 1. Insertion loss of Gore-Tex cable.

measurement system. A 3-foot length of Gore-Tex® cable with SMA connectors and a single APC-7 adapter on one end of the cable has been tested and utilized with the probe measurement system with satisfactory results over the frequency range examined (2-4 GHz).

2. Effects of Fluid Accumulation and Probe Contact Pressure

The possible effects of excessive fluid accumulation in the vicinity of the measurement probe have been a concern in assessing and assuring the accuracy of in-vivo dielectric property measurements [3]. The accumulation of fluid around and on the tip of the probe influences both the measurement accuracy of the probe and the repeatability of the measurements. Fluid accumulation around the probe after good contact between the probe tip and the measurement surface had been established only slightly influenced the measured data for high-loss tissues (brain surface and muscle) but greatly influenced the results obtained for low-loss tissue (fat). More significant was the accumulation of fluid on the tissue prior to contact with the probe, regardless of tissue type. The plot of the phase of the measured reflection coefficient presented in Figure 2 shows the effect of fluid accumulation in the measurement area prior to probe contact. These are raw data recorded on a swept-frequency basis using an X-Y recorder. Note the significant influence (25%) of the fluid on the accuracy of the measured phase angle and also note the general lack of repeatability in the measurement. After studying several methods to alleviate this problem on an a priori basis such that its presence would be either eliminated or accounted for, and therefore neglected, it was determined that the most effective means to prevent the influence of excessive fluid accumulation on measured results was to continuously monitor the condition of the measurement area and to continuously remove excessive fluid. The following approach has proven to be effective in solving the fluid accumulation problem:

1. The probe tip should be thoroughly cleaned between each measurement sequence. This cleaning prevents the buildup of any fluid residue which may have dried on the probe tip and which may act as an insulating layer between the probe tip and the tissue during subsequent measurements.

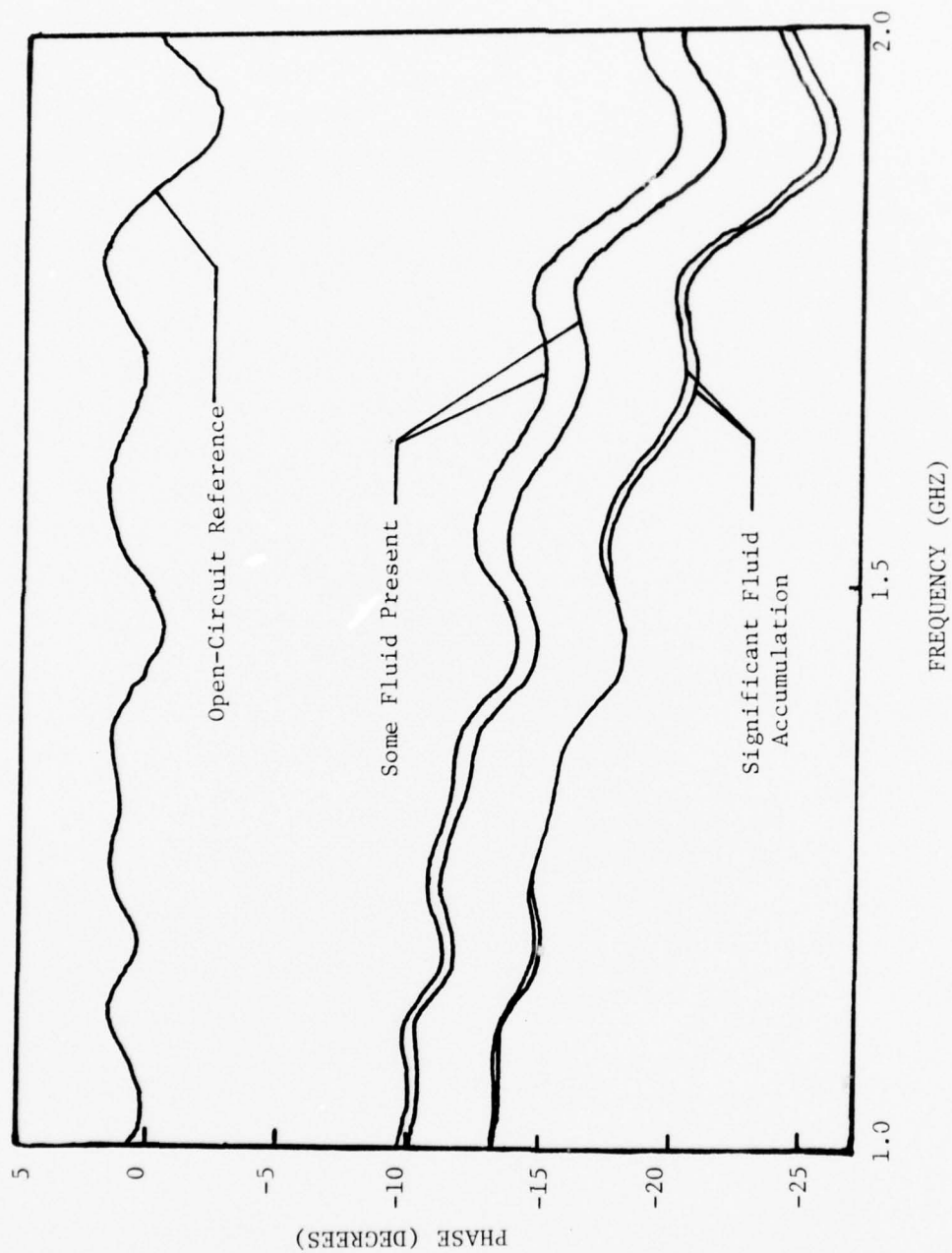


Figure 2. Phase of measured reflection coefficient for muscle under two conditions of fluid accumulation on tissue prior to measurement.

2. Adequate probe contact with the measurement area was found to be extremely important. Excessive contact pressure is not required to ensure good measurement results, but complete, uniform contact with the tissue is essential.
3. The buildup of excessive fluid in the measurement area or around the probe is best prevented by judicious use of cotton-tipped swabs and pledgets and 2-inch x 2-inch absorbent gauze pads. This simple procedure combined with continuous monitoring of the tissue's condition prevents fluid accumulation and seepage into the probe contact region of the measurement area.

Results of swept-frequency measurements where these procedures were observed are shown in Figure 3. Here the phase of the measured reflection coefficient is plotted as a function of frequency for four repeated measurements of the same tissue sample; the probe was completely removed from the sample and cleaned between each swept-frequency recording. The repeatability demonstrated by agreement of the four sweeps is excellent, and the dielectric values computed from the measured reflection coefficient phase and amplitude following systemic error correction (Section III) were accurate.

C. Frequency Range, Sample Volume, and Fabrication Considerations

There are numerous factors which influence the useful frequency range of the probe and the resulting measurement accuracy. Three of these factors (phase variation with cable flexure, fluid accumulation, and probe contact with the measurement area) were discussed in the preceding subsection. Here, the interactions among probe diameter, sample volume, probe fabrication techniques, and resultant useful frequency range are considered.

Several probe configurations have been evaluated during the first year of this research program and under a previous program supported by the Army [3]. Radiating probes with an extended center conductor of nearly 0.5-inch length and capacitative probes of infinitesimal length where only a fringing field exists have been fabricated and evaluated. The various probes have been constructed of semi-rigid coaxial cables whose diameters have ranged from 0.141 inch to 0.047 inch (approximately the diameter of a #18 hypodermic needle). The probes used in the

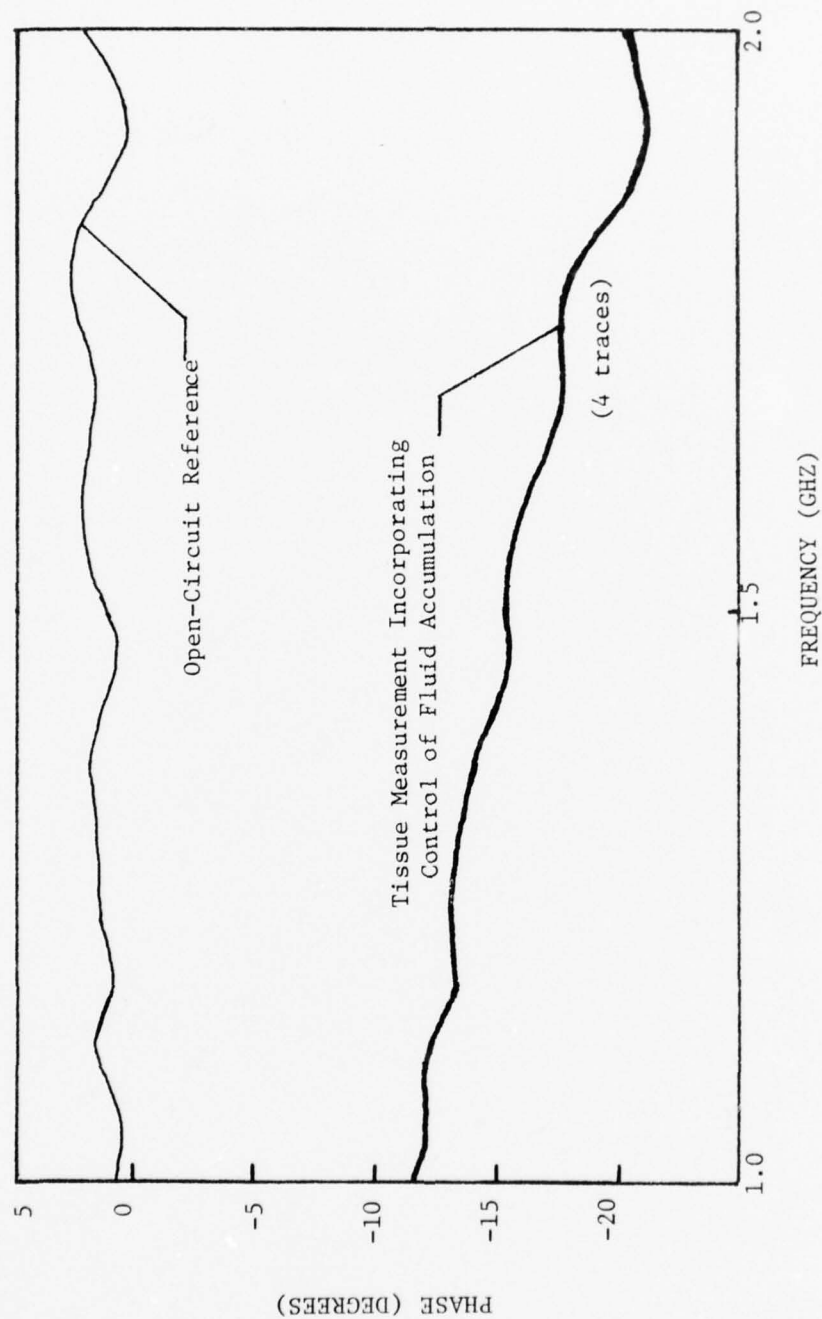


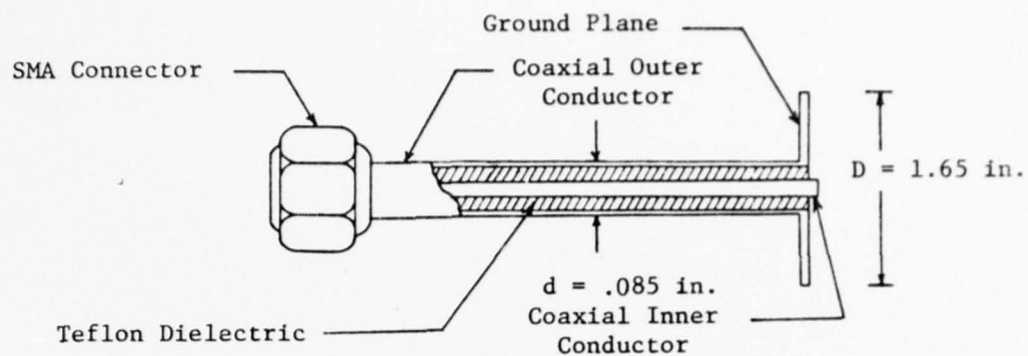
Figure 3. Phase of measured reflection coefficient for muscle under conditions where fluid accumulation was controlled. Data presented are four repeated measurements.

experimental investigations described in Section IV of this report were fabricated from 0.085-inch diameter semi-rigid coaxial cable. Infinitesimal probes with and without ground planes, as diagrammed in Figure 4, were used for the in-vivo measurements. However, in later experiments, far more extensive use was made of the probe without a ground plane.

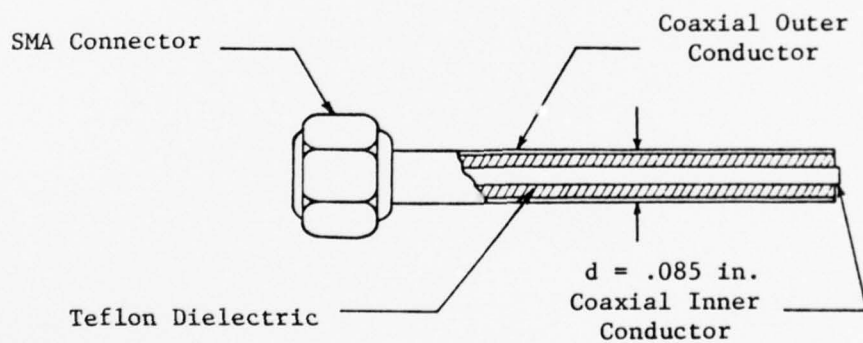
Methods for improved probe fabrication were investigated in terms of probe frequency response. The probes were fabricated from a section of open-ended semi-rigid coaxial cable. The quality of the connector attachment proved to be significant with respect to the useful frequency range for obtaining accurate results. It should be noted that the connector attachment on a 0.047-inch diameter probe limited the useful frequency range to 4 GHz as determined from dielectric measurements of deionized water, although such a small probe is theoretically useful to above 10 GHz. Therefore, the quality of the connector itself and its attachment to the probe are extremely important contributors to the ultimate accuracy and useful frequency range of the probe.

The in-vivo probe (Figure 4) is fabricated as follows. A section of open-ended semi-rigid coaxial cable with a slightly extended center conductor is selected. When necessary, a small circular ground plane is included to minimize fringing effects. The SMA connector is attached to the probe by first removing the center conductor and teflon dielectric material. The connector is then soldered to the outer conductor followed by reassembly of the probe using the center conductor as the center pin of the connector, thus avoiding additional soldering. In this manner, it is possible to attach the SMA connector without heating the teflon dielectric. While disassembled, the center and outer conductors of the probe are first flashed with nickel plating and then gold plated. Plating the probe with an inert metal, such as gold, greatly reduces chemical reactions between the probe and the electrolyte in the tissue. This process virtually eliminates oxidation of the probe's metallic surfaces and helps to minimize any possible electrode polarization effects.

Length and diameter also affect the useful frequency range of a given probe, and equally important, the minimum measurable sample volume



a) Monopole dielectric measurement probe with ground plane.



b) Monopole dielectric measurement probe without ground plane.

Figure 4. Two configurations of the monopole dielectric measurement probe.

as well. When the effective length of the probe in a dielectric material is greater than one-tenth wavelength, the probe antenna's current distribution changes in a manner dependent upon the dielectric material, and the impedance given by Equation (2) is no longer valid. The 0.5-inch long probe fabricated under a previous program [1] was useful over only a limited frequency range because its effective length increased by the square root of the dielectric constant of a material when inserted into that material. In that case (0.5-inch long probe), Equation (2) was not valid above 2.0 GHz for tissues such as muscle and kidney. Even at an effective length of one-tenth wavelength, a radiation field from the probe exists. For the dielectric properties of a material to be accurately measured, it is necessary that the entire radiation field be contained within the sample. If the sample volume does not entirely contain the probe's field, errors introduced in the measurement of the antenna terminal impedance can be expressed quantitatively by use of the reaction theorem [1,7,10]. For low-loss samples, the required sample volume can be considerable, but for samples having high loss, such as most biological tissues, it is possible to define a reasonable sample volume which contains the long probe's radiation field.

For short monopole probes whose center conductor approaches zero length, the terminal impedance is entirely reactive (Equation (3)), and only the probe's fringing field is present. Thus, for very short (infinitesimal) probes, the minimum sample volume required for accurate dielectric measurements is defined by the fringing field, which in turn is primarily dependent upon the distance between the tightly-coupled center and outer conductors of the probe. Using 0.085-inch diameter probe, the measured dielectric properties of water and methanol varied less than one percent over the 0.5-10 GHz frequency range for sample volumes ranging from 15 ml to 250 ml. These results are detailed on pages 50 and 51 of Reference 3. In fact, less than 20-percent changes in computed dielectric properties were observed over the same frequency range when results from a 50-ml sample volume of water was compared to a single drop of water suspended from the end of the 0.085-inch diameter

probe. Figure 5 shows the relationship between the minimum sample volume required for accurate results and probe diameter for infinitesimal probes having a totally reactive impedance. As noted in Figure 5, the plotted relation between sample volume and probe diameter applies to medium- and high-loss dielectrics which includes all biological tissues -- even fat. When very low-loss samples (such as paraffin) are measured, significantly larger sample volumes (than those in Figure 5) would be required. Finally, it should be noted that the upper frequency for which the relationship in Figure 5 is valid also depends upon the probe diameter. The maximum usable frequency range of the probe is decreased as the probe diameter is increased because with increasing probe diameter and frequency, the probe impedance is no longer entirely reactive and a radiation field exists.

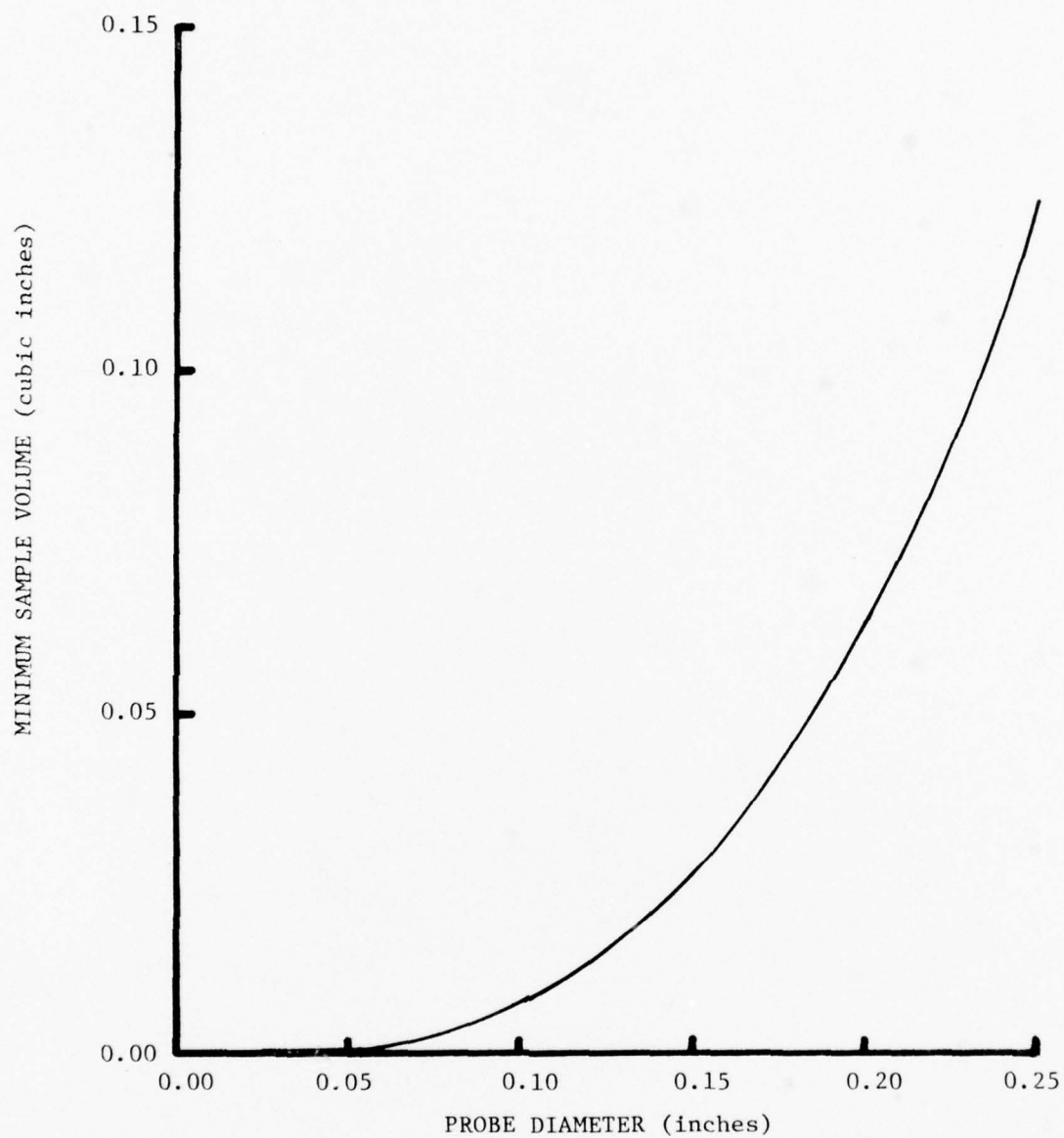


Figure 5. Minimum sample volume required for accurate dielectric property determination as a function of probe diameter for the infinitesimal probe. This relationship is valid only for medium- and high-loss samples.

SECTION III

MEASUREMENT SYSTEM DEVELOPMENT

Network-analyzer-based instrumentation is being used on this research program to perform in-vivo probe dielectric measurements. The development of this instrumentation required several years of careful design and testing with major difficulties being encountered in the areas of hardware (expense and suitability), data acquisition (accuracy and speed), and data processing (complexity). In its present form, the instrumentation utilizes a semi-automated network analyzer system that features automatic, computer-controlled data acquisition and data processing. The computer routine for data processing has the capability to convert the raw measured data from the network analyzer to the desired dielectric property information. In addition, the data processing routine contains an error correction subroutine that can be used to minimize the effects of systemic errors inherent in network analyzer measurements. This subroutine is based on the vector error-correction technique developed by Hewlett Packard [11]; however, several modifications have been added to make it better suited for applications utilizing the in-vivo probe.

In the remaining portions of this section, the network-analyzer-based instrumentation and the vector error-correction technique are discussed in further detail. The results of tests performed to evaluate the suitability of the instrumentation and effectiveness of the data processing routines are also discussed.

A. Network-Analyzer-Based Instrumentation

1. Hardware

A Hewlett Packard network analyzer system is the central component in the instrumentation being utilized in the in-vivo probe measurements. The network analyzer system measures the complex terminal impedance of the in-vivo probe in the form of the complex reflection coefficient. A block diagram of a manually operated version of this instrumentation used in two preliminary experiments performed on this

program is depicted in Figure 6. This figure shows that a section of low-loss flexible cable is used to attach the in-vivo probe to the reflection test unit. The reflection test unit is essentially a reflectometer which samples the incident and reflected RF signals at the in-vivo probe. The ratio of these two sampled RF signals is directly proportional to the complex reflection coefficient of the in-vivo probe. The two sampled RF signals are then directed into the two input ports (REFERENCE and TEST) of the network analyzer's frequency converter where the RF frequency is translated to an intermediate frequency of 278 kHz. The intermediate frequency (IF) signals retain the same relative amplitude and phase relationships that existed between the two original RF signals. The IF signals are then fed into the network analyzer which computes their complex ratio. Two DC voltages proportional to the amplitude and phase of this ratio are accessible through two ports on the rear panel of the network analyzer. A digital voltmeter is used to measure the value of these amplitude and phase voltages. By normalizing the voltages measured for the in-vivo probe to voltages measured for a known termination (e.g., a short circuit or open circuit), the complex reflection coefficient of the in-vivo probe can be computed. The value of this parameter, along with the appropriate frequency and probe characteristics (i.e., the free-space capacitance of the probe), is then inputted into a computer program to compute the dielectric properties.

The manual version of the instrumentation was used in the preliminary experiments as a matter of convenience. For example, the manual version permitted some initial measurements to be performed at the Emory University Medical School, Department of Physiology without creating a logistics problem. However, subsequent in-vivo probe measurements have been made at Georgia Tech using the semi-automated instrumentation. A block diagram of the latest version of the semi-automated instrumentation is shown in Figure 7. It is apparent that this instrumentation is significantly more complex than the manual system, and in fact, a great deal of effort has been expended in the development of the hardware and software utilized in the semi-automated instrumentation. However, additional benefits such as computer-controlled measurements, automatic data acquisition and data processing

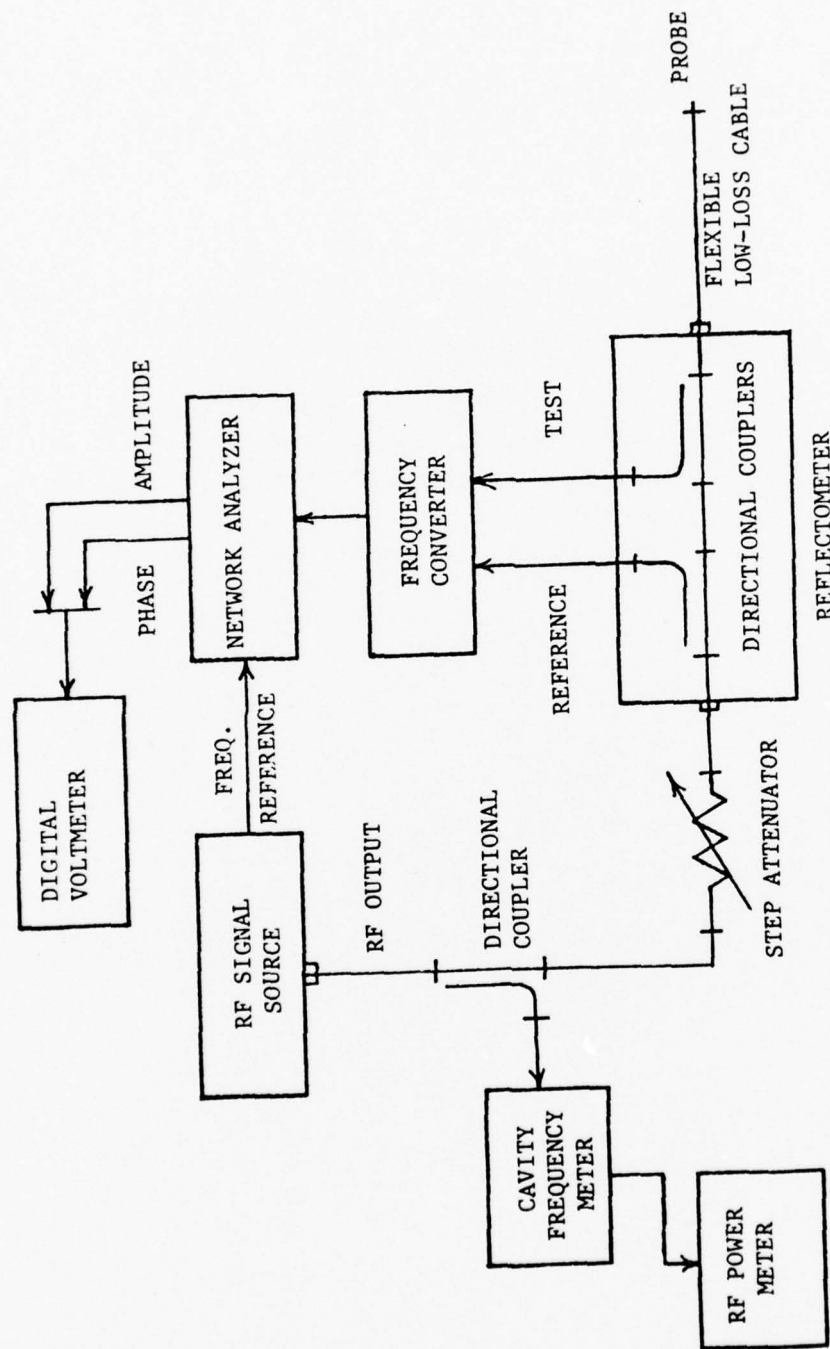


Figure 6. Block diagram of manually-operated in-vivo probe measurement system used in the initial experiments.

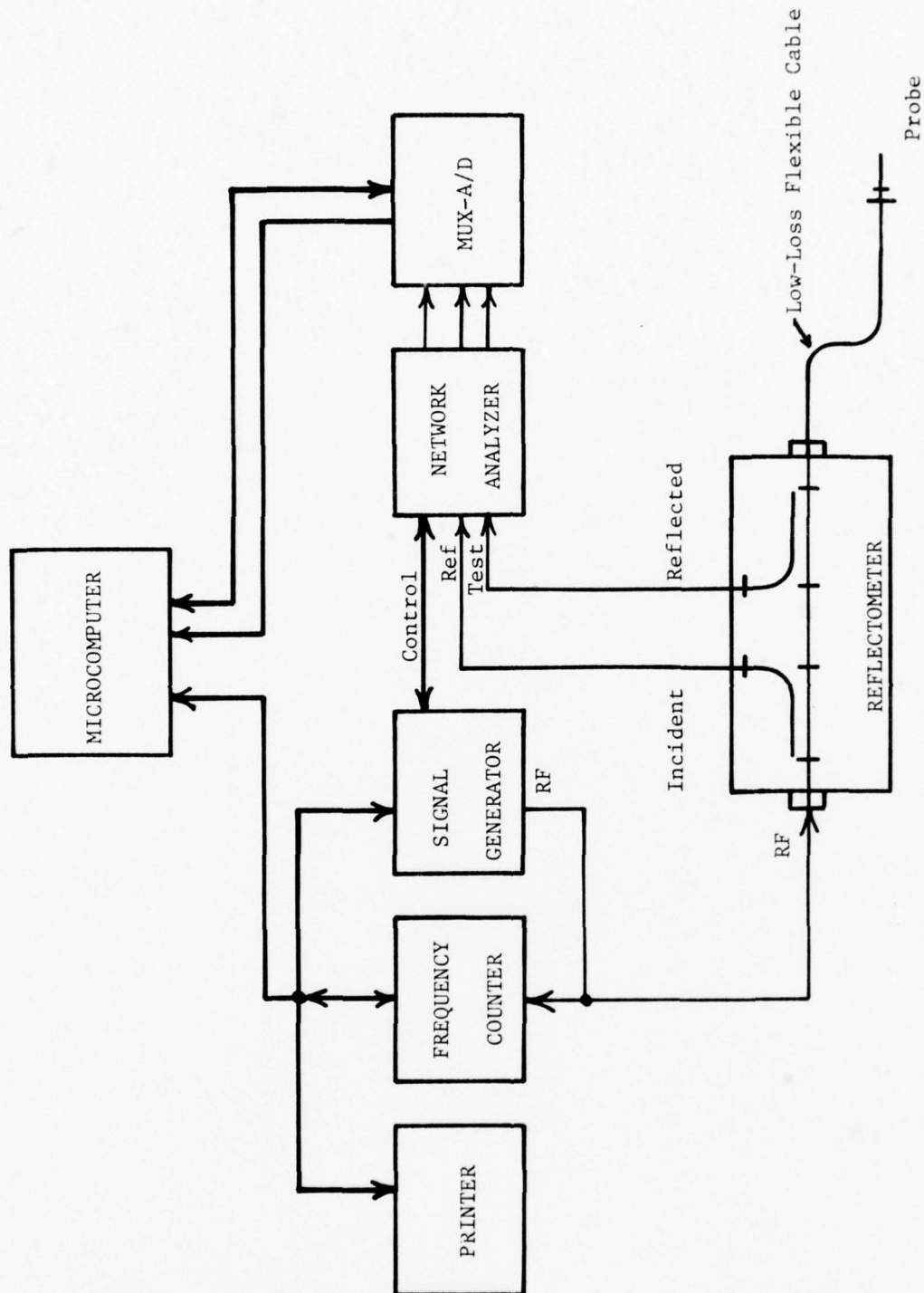


Figure 7. Block diagram of the present semi-automated data acquisition/data processing in-vivo probe measurement system.

(including vector error-correction), and an ability to perform measurements essentially on a real time basis have more than justified this expense.

Figure 7 shows that the Hewlett-Packard network analyzer is the major component in the semi-automated instrumentation as well as in the manual system. However, the computer depicted at the top of Figure 7 is also a key system component. The computer presently being utilized is a stand-alone desk-top model (Commodore PET-Model 2001-8) which has several features that make it well suited for these types of applications. These features include two I/O ports (for interfacing the PET with peripheral devices), a 1000-character CRT display (for printing out user directed prompts), and built in cassette storage (for storing program or data files). It has a resident BASIC interpreter, can be alternatively programmed directly in machine code, and has a powerful feature that allows mixed mode programming when desired (i.e., a single program can contain both BASIC and machine routines). Notably, one of the PET's two I/O ports has been set up according to IEEE Standard 488-1975, which permits the PET to communicate with multiple peripherals through its single IEEE port. As indicated in Figure 7, full use is made of this IEEE port with three different devices: a programmable signal generator, a programmable frequency counter, and a printer. The signal generator provides the basic RF signal utilized in the dielectric property measurements, and the frequency counter measures the RF frequency of the signal supplied by the signal generator. The PET utilizes the frequency information outputted by the frequency counter as feedback data to exactly set the frequency of the signal generator to a user-specified value. The printer provides the system user with a hard copy of all measurement results.

The operation of the network analyzer portion of the instrumentation is nearly identical to the procedure described in the summary of the manual system. However, the complex reflection-coefficient information is provided in the form of three DC signals (AMPLITUDE, HORIZONTAL, and VERTICAL) that are proportional to the amplitude, horizontal component, and vertical component, respectively,

of the complex reflection coefficient. It should be noted that the PHASE signal is not measured as in the manual system. Instead, the phase of the complex reflection-coefficient is computed by taking the arctangent of the ratio of the VERTICAL and HORIZONTAL signals. By measuring phase in this manner, the ambiguity associated with cycling of the phase information each 360 degrees in direct phase measurements is avoided.

The combination multiplexer/analog-to-digital (MUX/AD) converter, shown in Figure 7, converts the AMPLITUDE, HORIZONTAL, and VERTICAL signals into binary (two's complement) signals suitable for inputting into the PET through the PET's second I/O port. The MUX/AD used in the system is a subminiature, microprocessor-compatible unit manufactured by Analogic (Model MP-6812), and it can accept up to 16 separate analog signals which can individually be multiplexed to an internal 12-bit AD converter. A more detailed wiring diagram of the interconnections between the PET and the MUX/A-D is shown in Figure 8.

Various machine language routines were implemented in the computer so that it could communicate with the MUX/A-D. BASIC language routines were implemented for communication with the other peripheral devices since the PET's resident interpreter is set up to automatically communicate with peripherals conforming to IEEE Standard 488-1975.

2. Software

Once the PET inputs and stores the binary forms of the AMPLITUDE, HORIZONTAL, and VERTICAL signals, it performs the sequence of operations necessary to compute the desired dielectric properties. This sequence of operations consists of the following steps:

- The binary data inputted from the MUX/AD are converted back into their analog equivalent;
- The analog equivalent values are compared to reference values and are used to compute the complex reflection coefficient of the in-vivo probe;
- The complex reflection coefficient values are converted into the form of a complex impedance;
- The complex impedance values are used to determine the desired dielectric properties; and

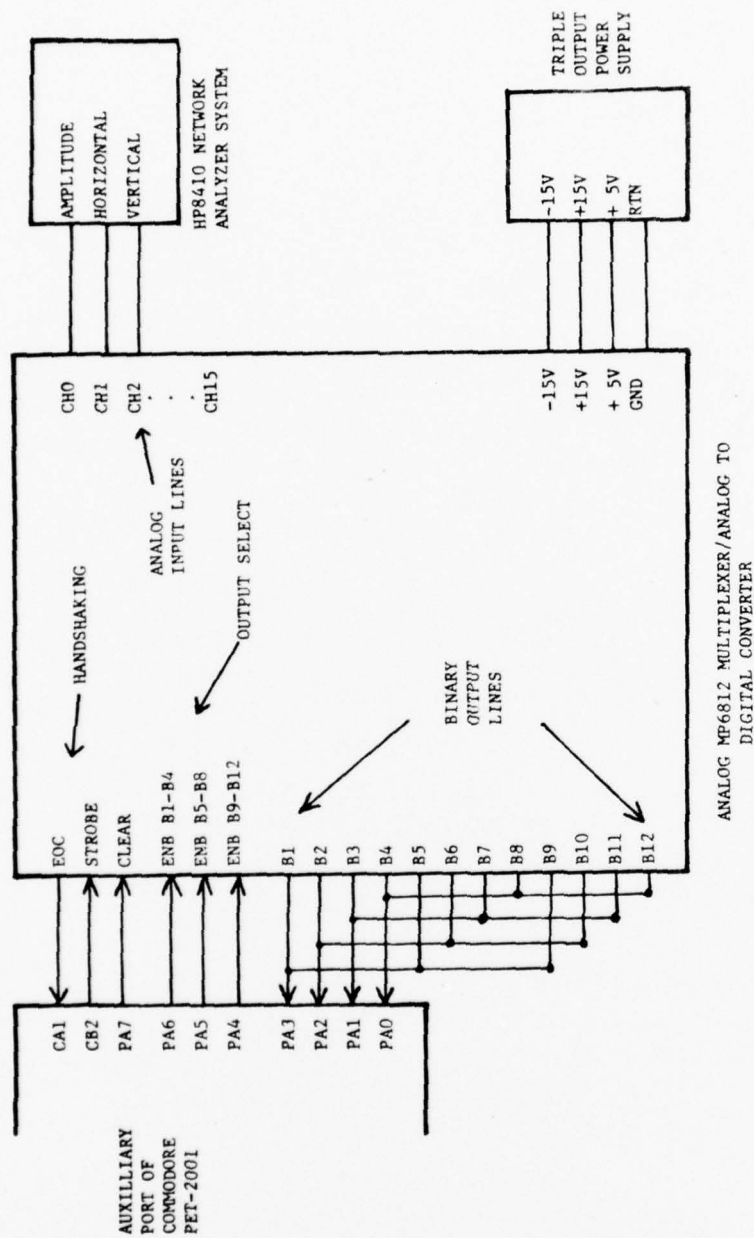


Figure 8. Wiring diagram of Commodore PET computer to analog combination multiplexer/analog to digital converter.

- The dielectric property values are then sent to the printer to provide the system user with a hard copy of the measurement results.

Two different computer algorithms were developed for use on this research program. Each program makes use of the PET's "mixed mode" programming capability. BASIC language instructions are used where complex computations are needed, and machine language instructions are used in the data acquisition process where speed is important. The first algorithm is used for performing single frequency measurements as a function of time. The second algorithm (referred to as the "swept-frequency" algorithm) is used for performing measurements over a specified frequency band. Flow charts of these two computer algorithms are depicted in Figures 9 and 10, respectively. The two algorithms have common features such as control of the operational sequence of the dielectric property measurement procedure, display of concise user-directed prompts (where appropriate), and complete processing of all raw data (including vector error-correction of systemic measurement errors). The algorithms also have features that make them unique from one another. For example, the flow chart in Figure 9 shows that the single-frequency algorithm can be set up in an "automatic mode" in which measurements are performed continuously at user-defined intervals that can be as short as five seconds. Another unique feature of the single-frequency algorithm is that a real time record of measurement time is maintained and printed out with the measurement results. A unique feature of the swept-frequency algorithm is its ability to automatically set the instrumentation to perform measurements at a sequence of user specified frequencies. As many as 21 equally spaced frequencies may be specified.

The majority of dielectric measurements performed on this research program will likely utilize the single-frequency algorithm to record data as a function of time. An example of measurements made using this algorithm is shown in Figure 11.

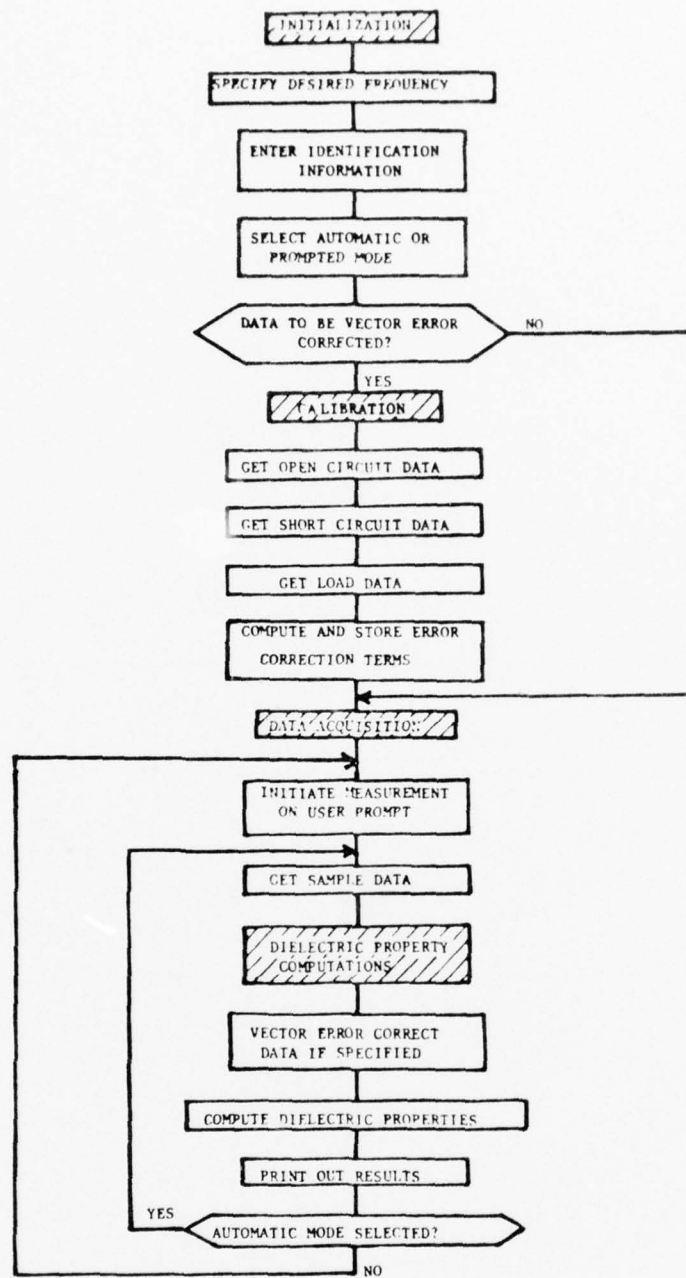


Figure 9. Flow chart of algorithm for single frequency measurements.

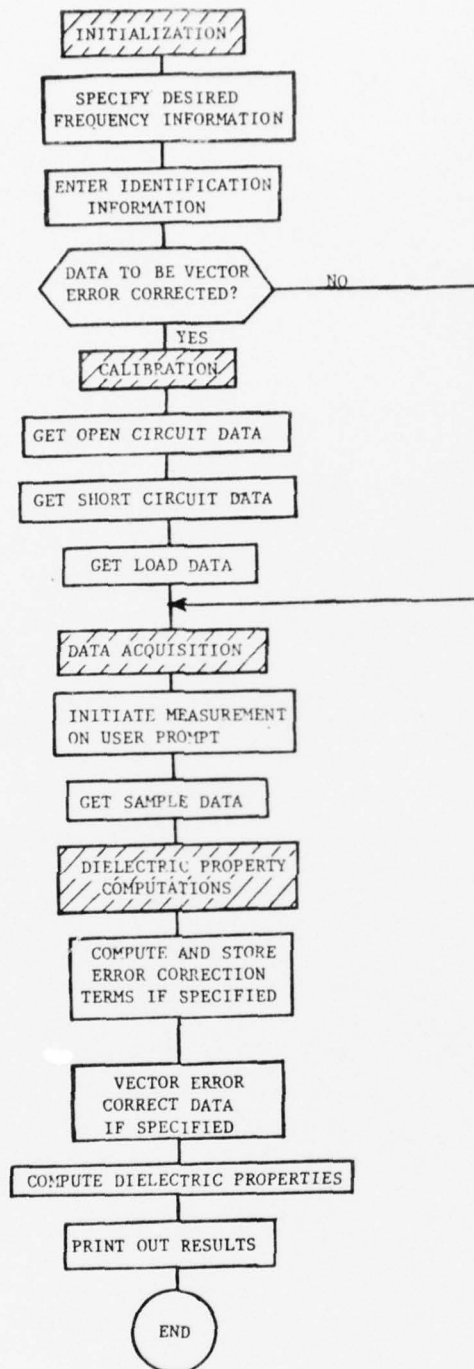


Figure 10. Flow chart of algorithm for multiple frequency measurements.

DP'S OF H2O(EO/FL3). 9/5/79. C0= 1.21E-14.

FREQ (MHZ)	AMP (DB)	THETA (DEG.)	DIELECTRIC CONSTANT	SIGMA (MMHO/CM)	LOSS TANG	TIME (H:M:S)
2450	-1.38	-72.9	78.53	17.89	.167	012026
2450	-1.38	-72.9	78.59	17.27	.161	012031
2450	-1.38	-73.14	78.88	17.94	.167	012036
2450	-1.38	-72.9	78.53	17.89	.167	012041
2450	-1.38	-72.9	78.53	17.89	.167	012046
2450	-1.38	-72.9	78.53	17.89	.167	012051
2450	-1.38	-73.14	78.88	17.94	.167	012056
2450	-1.38	-73.14	78.88	17.94	.167	012101
2450	-1.38	-72.9	78.53	17.89	.167	012106
2450	-1.38	-73.14	78.88	17.94	.167	012111
2450	-1.38	-73.14	78.88	17.94	.167	012116
2450	-1.38	-73.14	78.88	17.94	.167	012122
2450	-1.38	-72.9	78.53	17.89	.167	012127
2450	-1.38	-73.14	78.88	17.94	.167	012132
2450	-1.38	-72.9	78.53	17.89	.167	012137
2450	-1.38	-73.14	78.88	17.94	.167	012142
2450	-1.38	-72.9	78.53	17.89	.167	012147
2450	-1.38	-73.14	78.88	17.94	.167	012152
2450	-1.38	-72.9	78.53	17.89	.167	012157
2450	-1.38	-73.14	78.88	17.94	.167	012202
2450	-1.38	-73.14	78.88	17.94	.167	012207
2450	-1.38	-72.9	78.53	17.89	.167	012212
2450	-1.38	-73.14	78.88	17.94	.167	012217
2450	-1.38	-72.9	78.53	17.89	.167	012223
2450	-1.38	-73.14	78.88	17.94	.167	012228
2450	-1.38	-72.9	78.53	17.89	.167	012233
2450	-1.38	-73.14	78.88	17.94	.167	012238
2450	-1.38	-73.14	78.88	17.94	.167	012243
2450	-1.38	-73.14	78.88	17.94	.167	012248
2450	-1.38	-73.14	78.88	17.94	.167	012253
2450	-1.38	-73.14	78.88	17.94	.167	012258
2450	-1.38	-73.14	78.88	17.94	.167	012303

Figure 11. Sample printout of dielectric property data measured for deionized water using single frequency program in the automatic mode.

B. Microwave Measurement Error Correction and Calibration

Measurement errors associated with the network analyzer can be separated into two categories: instrument errors and test set/ connection errors. Instrument errors are measurement variations due to noise, imperfect conversions (in such equipment as the frequency converter), crosstalk, inaccurate logarithmic conversion, non-linearity in displays, and overall drift of the system. Test set/connection errors are due to the directional couplers in the reflectometer, imperfect cables, and the use of connector adapters. The instrument errors exhibited by the 8410B network analyzer are very small. Noise is specified to be less than -78 dBm equivalent input noise, and the isolation between channels is greater than 65 dB from 0.1 to 6.0 GHz and greater than 60 dB from 6.0 to 12.4 GHz. Reference and test channels track within ± 0.3 -dB amplitude and ± 1 degree phase over any octave band from 0.1 GHz to 8.0 GHz with only a slight degradation at 12.4 GHz. Drift is specified to be within ± 0.5 dB/ $^{\circ}$ C and $\pm 0.1^{\circ}$ phase/ $^{\circ}$ C. The primary source of measurement uncertainty is due to test set/connectors at UHF and microwave frequencies. These uncertainties are quantified as directivity, source match, and frequency tracking errors.

An analytical model for correcting test set/connection errors was implemented based on the model used by Hewlett-Packard for correcting reflectivity measurements on their semi-automatic network analyzer system [11]. This model was reported previously [3]; therefore, only the essentials of this model for vector error-correction are restated here. The three types of test set/connection errors (directivity, frequency tracking, and source match) accounted for by the model are shown schematically in Figure 12. The term S_{11m} is the measured reflection coefficient, and S_{11a} is the actual reflection coefficient. The directivity error E_{11} is due primarily to direct leakage of the incident signal into the reflected signal channel via the reflectometer directional couplers. The source match error E_{22} is caused by the re-reflection of the reflected signal back to the test port. $E_{21}E_{12}$, the frequency tracking error, is caused by small variations in gain and

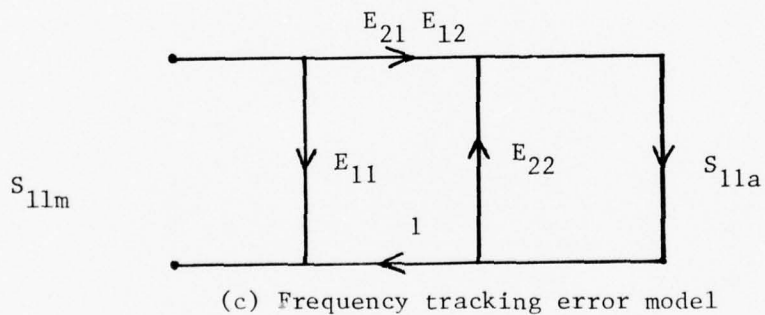
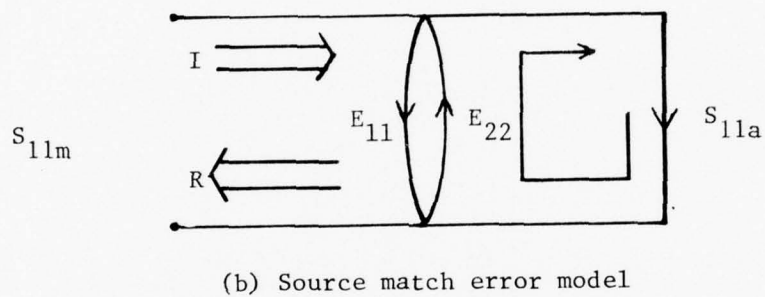
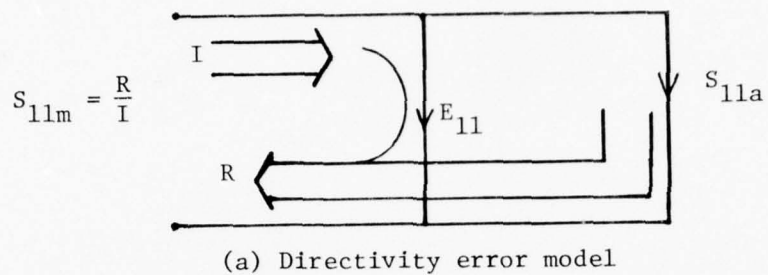


Figure 12. Error models used for test set/connection errors.

phase flatness between the test and reference channels of the analyzer as a function of frequency. These three error terms are determined by calibrating the system using three independent standard terminations each of whose actual reflection coefficient, S_{11a} , is known at all frequencies of interest. The measured reflection coefficient S_{11m} expressed as a function of the error terms and the actual reflection coefficient S_{11a} is

$$S_{11m} = E_{11} + \frac{S_{11a} + (E_{21}E_{12})}{1 - E_{22}S_{11a}} \quad (4)$$

The directivity error E_{11} is determined by measuring a sliding matched load termination. Because no matched load is truly perfectly matched, multiple load measurements for a number of different path lengths are made. The loci of these points form a circle whose center is the true directivity error vector. The remaining error terms are determined in like manner through the solution of Equation (4). A short circuit ($S_{11a} = 1 \angle -180^\circ$) termination and an open circuit ($S_{11a} = 1 \angle 0^\circ$) termination provide the two necessary conditions for determining E_{22} and $E_{21}E_{12}$. Once the measurement error terms are known at each frequency, S_{11a} can be determined from S_{11m} . Solving Equation (4) for S_{11a} , one obtains

$$S_{11a} = \frac{S_{11m} - E_{11}}{E_{22}(S_{11m} - E_{11}) + E_{21}E_{12}} \quad (5)$$

Equation (5) is implemented in the error correction algorithm which is part of the data processing software on the microcomputer system. Once the measured data are corrected, the remaining data processing software computes the dielectric properties of the test material.

C. Evaluation of System Performance

The semi-automated data acquisition/data processing system and the systemic measurement error correction algorithm have been tested and evaluated through measurements of terminations having known reflection

coefficients and through repeated measurements of materials of known dielectric properties. In both types of tests, the sample impedance data were measured in the form of a complex reflection coefficient. To test the systemic measurement error correction capability of the complete system, reflection coefficient data were first measured for known terminations which included a short circuit, an open circuit, and a sliding matched load at five different positions. These measurements were performed at two different reference planes -- the APC 7mm connector on the reflectometer and the SMA connector/adaptor to which the probe is attached -- to determine the correction needed in the measured sample reflection coefficient to account for test set/connection errors. The results of these measurements indicated that calibration at the SMA port and at the end of the probe provided a better accounting of systemic measurement errors. The open- and short-circuit data were measured at the end of the probe itself and the load measurements were made at the SMA connector/adaptor. The results of a test of the error correction model are shown in Figure 13 where a short circuit was used as a sample test case following error correction at the probe/SMA connector reference planes. A short circuit termination was used as a sample because its reflection coefficient is accurately known and because it provides a check of the calibration data used in the systemic error correction model. As seen in Figure 13, a significant improvement is obtained with the vector error-correction as opposed to no correction for systemic measurement errors. Any remaining variations are due to residual directivity errors at the SMA connector or to instrument errors (0.3 dB amplitude, ± 1.0 degree phase) specified by the manufacturer of the network analyzer.

Measurements of deionized water and methanol were also performed to assess the overall measurement system accuracy. It is known from previous characterization of the dielectric properties of these materials that the data form a smooth curve [2,4,12-14]. Therefore, the vector error correction model should remove variations due to systemic errors with the resultant data forming a smooth curve in good agreement with reference data. The previously described software was used to (1)

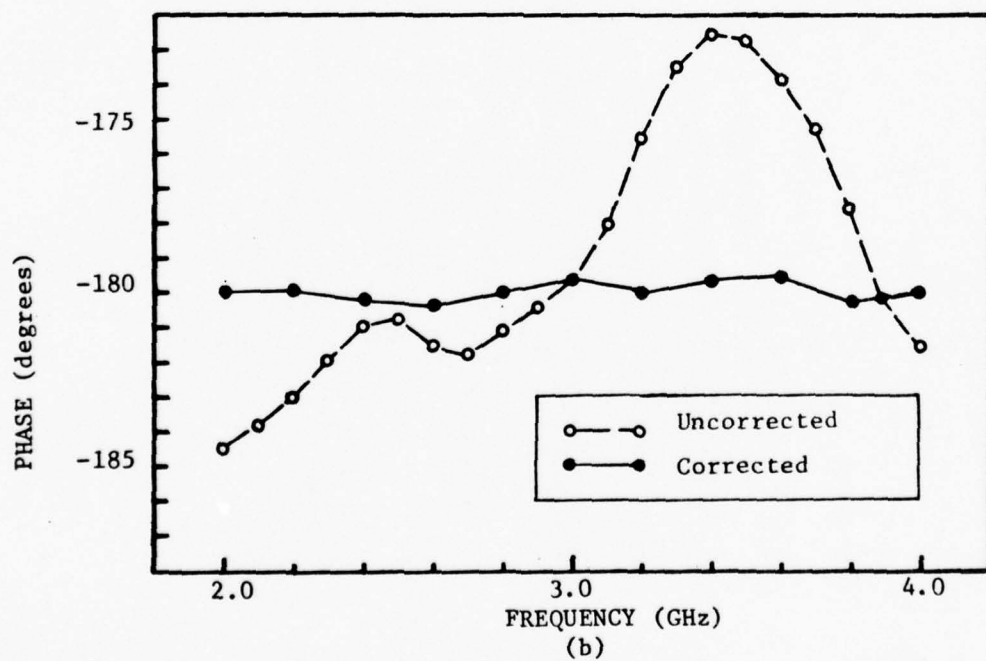
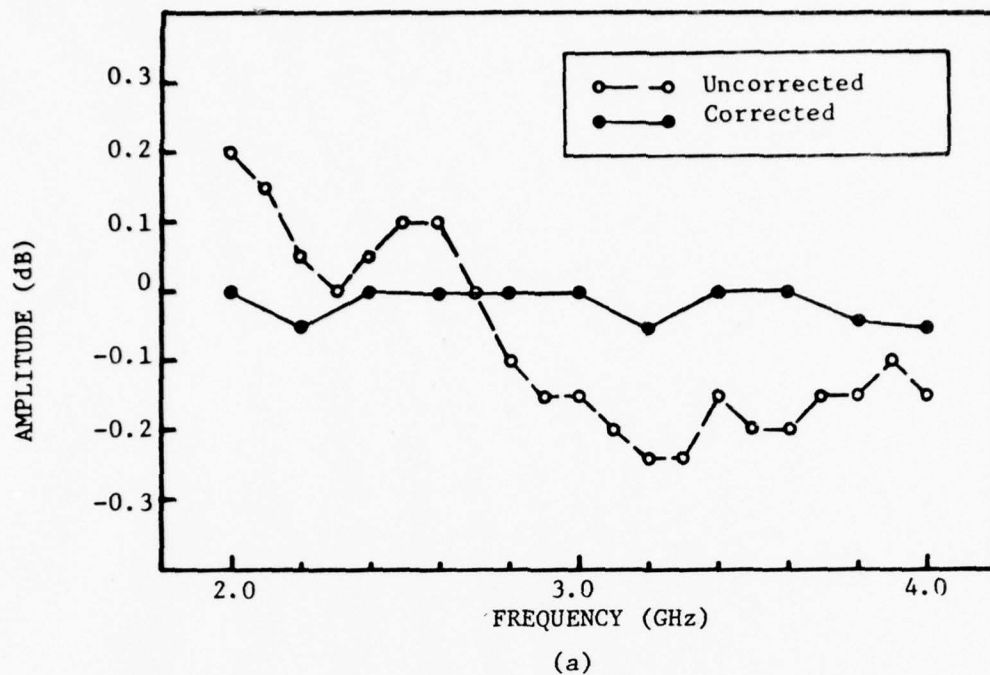


Figure 13. (a) Amplitude and (b) Phase of corrected and uncorrected short circuit termination reflection coefficient data.

acquire the sample data, (2) compute the various systemic measurement error terms (directivity, source match, frequency tracking), (3) compute the actual corrected reflection coefficient (S_{11a}), and (4) compute the desired dielectric properties (dielectric constant, conductivity, loss tangent) from the corrected reflection coefficient data. The computed relative dielectric constant and loss tangent for corrected and uncorrected water and methanol over the 1-7 GHz frequency range are shown in Figures 14 and 15, respectively. In both cases, these data show a considerable reduction in variability following systemic error correction. Correction of the systemic measurement errors places the results to within 3-4 percent of reference data.

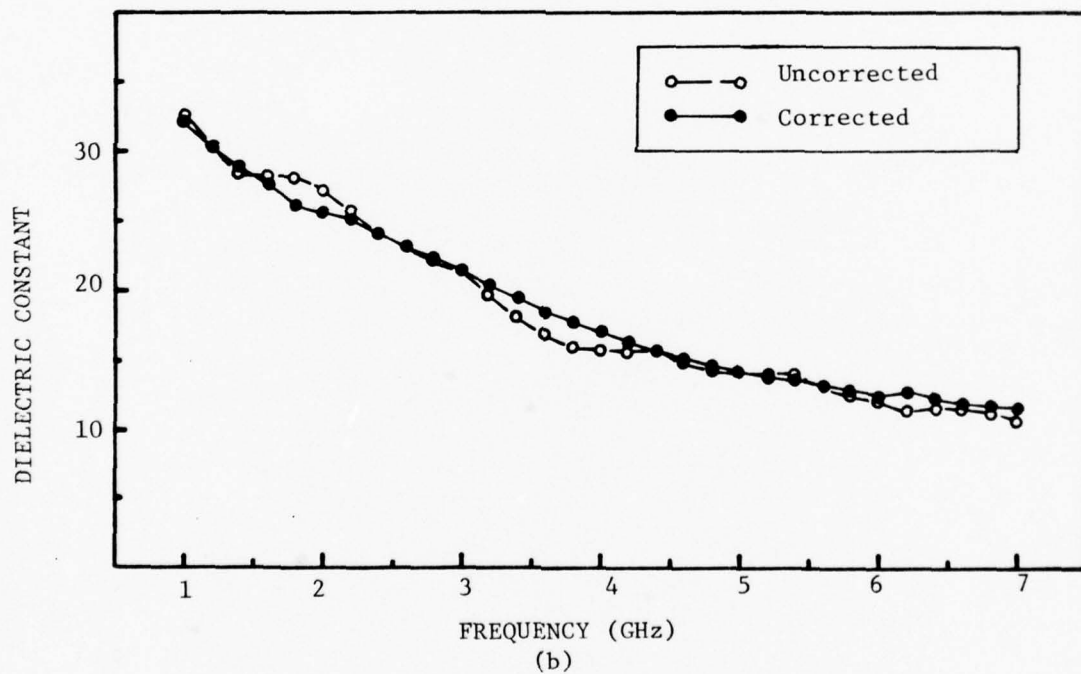
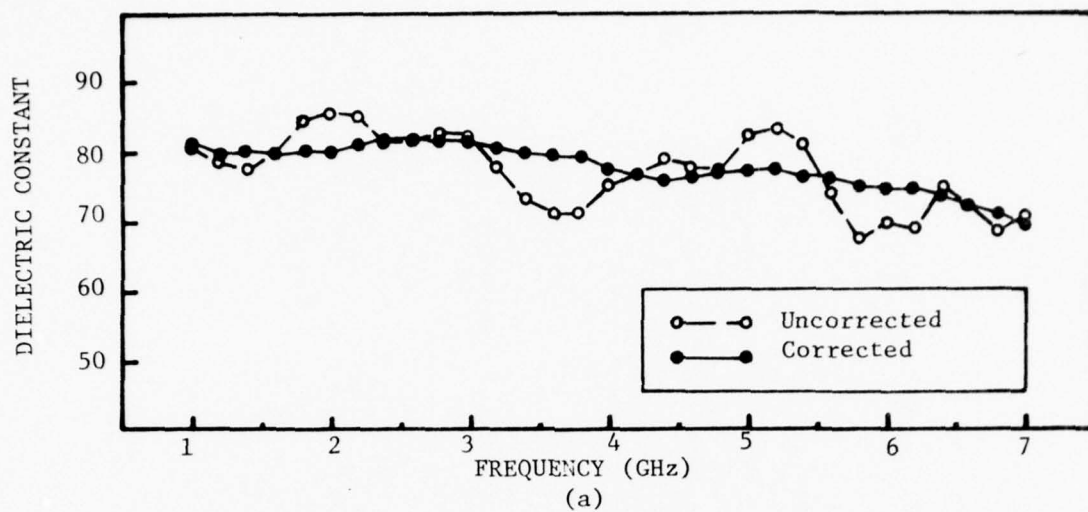


Figure 14. Relative dielectric constant of (a) water and (b) methanol measured at a temperature of 20°C with and without systemic error correction.

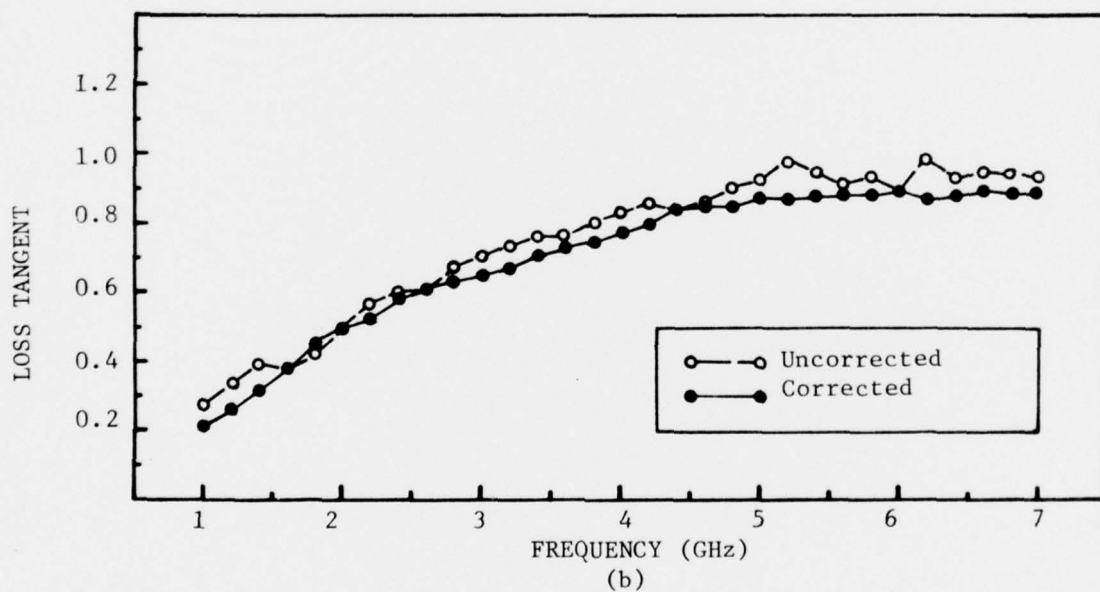
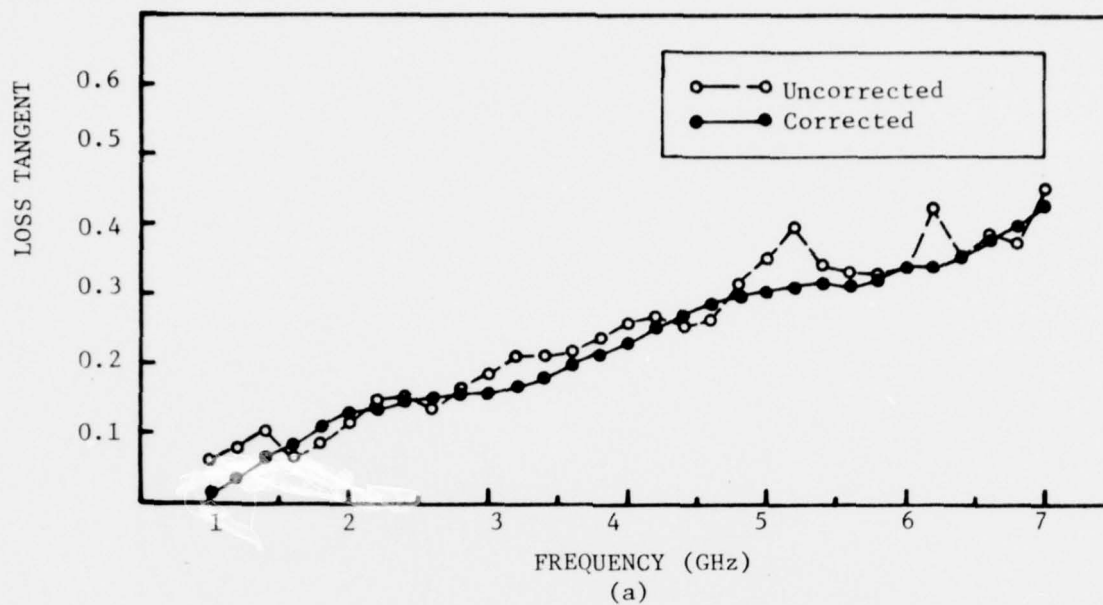


Figure 15. Loss tangent of (a) water and (b) methanol measured at a temperature of 20°C with and without systemic error correction.

SECTION IV

EXPERIMENTAL INVESTIGATIONS

This section summarizes the experimental investigations conducted during the first year of this two-year research program. The first part of this section describes the equipment and procedures associated with the physiological aspects of the experiments. The in-vivo probe and associated instrumentation used for the acquisition and processing of dielectric property data were described in Section II and III. The second part of this section outlines the procedures followed during experiments on dogs. The last part of this section presents the results of the experimental investigations.

A. Physiological Instrumentation and Surgical Equipment

In order to accomplish the required tasks for this research program, several items of specialized equipment were obtained either through purchase or as Government Furnished Equipment (GFE). Part of the equipment is necessary to expose surgically the brain of the experimental animal, whereas the remainder of the equipment is necessary to measure and to record physiological parameters.

In order to reliably perform surgical and measurement procedures, a method for securely holding the head of experimental animals is needed. As a result of this need, a David Koph Model 1504 Stereotaxic unit for dogs and monkeys was obtained as GFE from the Walter Reed Army Institute of Research (WRAIR). The device clamps the head by means of a mouthpiece, two eye bars, and two ear bars. The resulting stable, fixed position of the head greatly improved our ability to perform the surgical exposure of a preselected area of the brain. An illustration of a dog's head held in place using the stereotaxic is shown in Figure 16. In preliminary experiments, this surgery was difficult because the head was not supported; subsequently, however, a head support device made in the Georgia Tech machine shop permitted the surgery to be more easily accomplished. That head support device consisted of a grid of bars which were inserted into the dog's mouth, and then the dog's snout

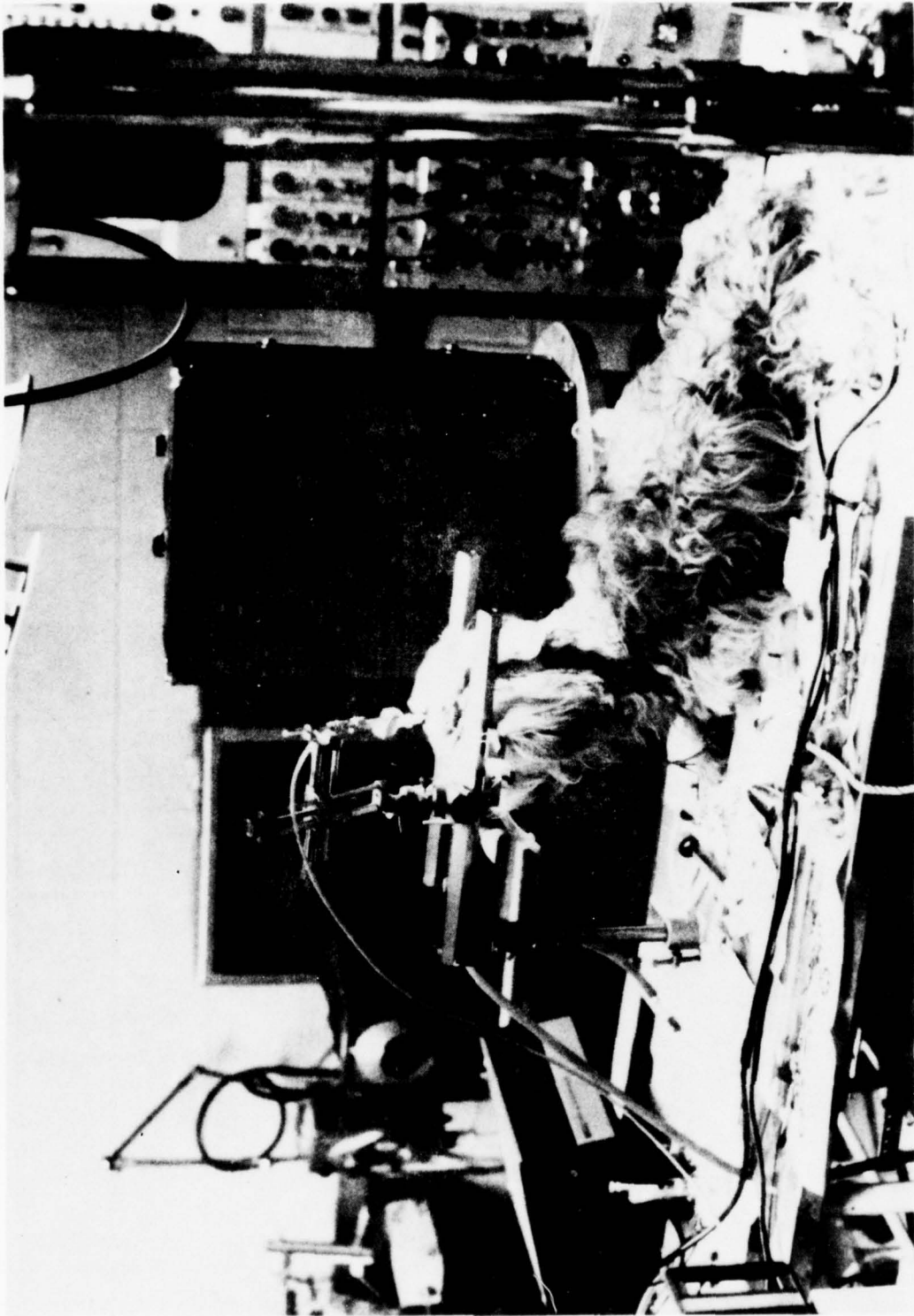


Figure 16. View of experimental animal positioned in stereotaxic apparatus for recording dielectric and physiological data.

was taped tightly shut. The support provided by the Georgia Tech device facilitated the surgery relative to the no-support case; however, the David Kopf stereotaxic unit now used is far superior. The stereotaxic unit also has coordinate scales which can be used to position accurately the measurement probe.

The animal surgery is accomplished both with surgical instruments available in the Biomedical Research Laboratory and with surgical instruments purchased on this program. In addition to general-purpose instruments, several special instruments for the exposure of the brain were obtained. These include a 1/2-inch trephine, rongeurs, and bone curettes. These instruments are used in our surgical laboratory.

A Foregger Rotameter anesthesia machine was also obtained as GFE from WRAIR. This device will serve two major purposes in later experiments. First, the anesthesia machine will be used to provide a breathing atmosphere of controlled composition in experiments in which blood flow to the brain will be increased by increasing the CO_2 content of the breathing atmosphere. Secondly, the anesthesia machine will be used to deliver gases with anesthetic and analgesic properties to the experimental animal. This procedure will eliminate the undesired secondary effects of using a barbiturate anesthetic. The anesthesia machine is currently being modified to perform these functions.

An instrument which measures the pH and the partial pressures of oxygen (P_{O_2}) and carbon dioxide (P_{CO_2}) in blood has been purchased for use on this research program. The basic instrument is a Radiometer PHM73 pH/Blood Gas Monitor which can measure the three parameters simultaneously. This device is very accurate in the physiological ranges of the parameters measured and has both a digital readout and an analog voltage output for each parameter. In this system, as it is used during the experimental investigation, the four sensing electrodes of the pH/Blood Gas Monitor are inserted into a Radiometer Flow Cuvette Assembly DS 67101. In the flow cuvette, which is made of glass, the electrodes' sensing elements come into contact with blood flowing through a tube. The electrodes and the flowing blood are surrounded by a separate chamber used as a water bath to maintain the temperature of the blood near 37°C .

There are now three major recording devices in the surgical laboratory. The first, a Narco Bio-Systems Physiograph Model DMP-4B, is a stripchart recorder with three channels for analog data and one channel for a time signal. In addition, the physiograph includes two blood pressure transducers and one EKG transducer, all with associated amplifiers. The output signals of these three transducer units are directly connected to the three analog channels of the recorder.

Two other instruments serve as auxiliary recording devices which can be connected to selected signals. A Sanborn Model 769 Oscilloscope with inputs through Sanborn 779 Amplifiers can display up to six channels of data simultaneously. Because of its large screen, this device is useful for observing blood pressure and EKG during surgery. An Offner Electronics Type RMC Dynograph is a six-channel stripchart recorder. It was necessary to build an adapter consisting of six buffer amplifiers for this recorder in order to interface with the voltage signals available from the transducers. This recording device is used to record up to six variables simultaneously.

B. Laboratory Procedures

The preparation of the animal for probe measurements of the brain involved several separate procedures. The dogs used in the experimental investigations performed during the first year were obtained from Emory University. The first step in each experiment was to anesthetize the animal at Emory with an injection of pentobarbital sodium (Nembutal) into a saphenous vein. The animal was then transported to the laboratory where measurements were performed. For the first two preliminary experiments, the animal was taken to a laboratory at Emory; for later experiments, the animal was transported to the surgical laboratory at Georgia Tech. Upon its arrival in the laboratory, the animal's state of anesthesia was checked, and a supplemental dose of anesthetic was given if necessary. Additional supplemental doses were administered throughout each experiment as required to maintain the desired level of anesthesia for the surgical and experimental procedures.

The surgical procedures began with exposure and cannulation of the femoral artery and vein on one side. The cannulae were connected to pressure transducers to measure arterial and venous blood pressures. Attempts were made in the first preliminary experiment to use a common carotid artery and an external jugular vein for these measurements. This procedure was abandoned because of the increased time required for exposure and cannulation of these vessels and because of the interference of cannulae in the neck with the head manipulations required later.

The next procedure was to establish the extracorporeal circuit of blood through the flow curvette. This procedure was not performed during the two preliminary experiments at Emory. In the first experiment at Georgia Tech, the circuit was attempted between a common carotid artery and an external jugular vein. However, this procedure was not used in other experiments for the same reasons that it was not used for blood pressure cannulations. In subsequent experiments, the femoral artery and vein on the opposite side from those cannulated for blood pressure were exposed and cannulated for the extracorporeal circuit. It was found that pretreatment of the tubing in the circuit with heparin was necessary to prevent immediate clotting. Occasional intravenous (IV) administration of heparin during the experiment insured a continuous flow of blood.

After the cannulations were completed and, in later experiments, the extracorporeal circuit established, the procedure to expose the brain began. Since the animal was on its dorsal surface for the cannulations, the animal was first turned onto its ventral side. In the first two preliminary experiments, the surgical procedure to expose the brain started at this point. In later experiments, the head was next placed into a holding device, which, most recently, was a David Koph stereotaxic. The skin and top layers of muscle were cut with a single midline incision extending from the eyes to 2-3 centimeters behind the lamboidal ridge. The underlying muscle tissue on the right side of the head was reflected by alternately scraping the tendinous tissue near the midline with a bone curette or sharp septum elevator and pulling the

muscles laterally. A hole was then drilled through the cranium using a 1/2-inch trephine. Bone wax was frequently inserted into the circular groove cut by the trephine to control bleeding from the bone. In all but the last experiment, the center of the hole was located midway between the eyes and the lamboidal ridge and approximately two centimeters from the midline. Also, in these experiments, the 1/2-inch diameter hole was adequate for the measurements performed. In the last experiment, the trephined hole was located over the medial ectosylvian gyrus and was enlarged using rongeurs to expose most of the gyrus.

Two general types of probe measurements were made during the experiments. In-situ dielectric measurements were made on the surface of the dura mater which was exposed by removal of the bone. In several cases, it was necessary to control the leakage of fluid onto the surface of the dura with small cotton pledgets around the edges of the hole. In-situ measurements were also made on the surface of the brain directly, or, more accurately, through the pia mater, after the dura was removed. After the cerebrospinal fluid drained from the area, there was little problem with fluid leakage and minimal control was required. Probe contact itself seemed to increase the leakage of fluid into the exposed dural and pial surfaces, perhaps due to the contact pressure of the probe with the measurement surface. If extraneous fluid was present before a measurement, the fluid was removed by brushing the area lightly with a wisp of cotton. The amount of fluid on the surface to be contacted by the probe was observed throughout the experiment, and data were rejected if fluid was present during a measurement. This procedure provided assurance that measurements were being made of the tissue and not of any overlying fluid.

The probes were held against the exposed tissue by hand in initial experiments. Contact pressure was classified as light, medium, or hard by the holder. Contact pressure seemed to influence the result of a measurement, but in no obvious pattern. In later experiments, the probe was held by the electrode carrier attached to the stereotaxic frame as shown in Figure 17. This configuration provided reproducible positioning of the probe and consistent contact pressure. Since the

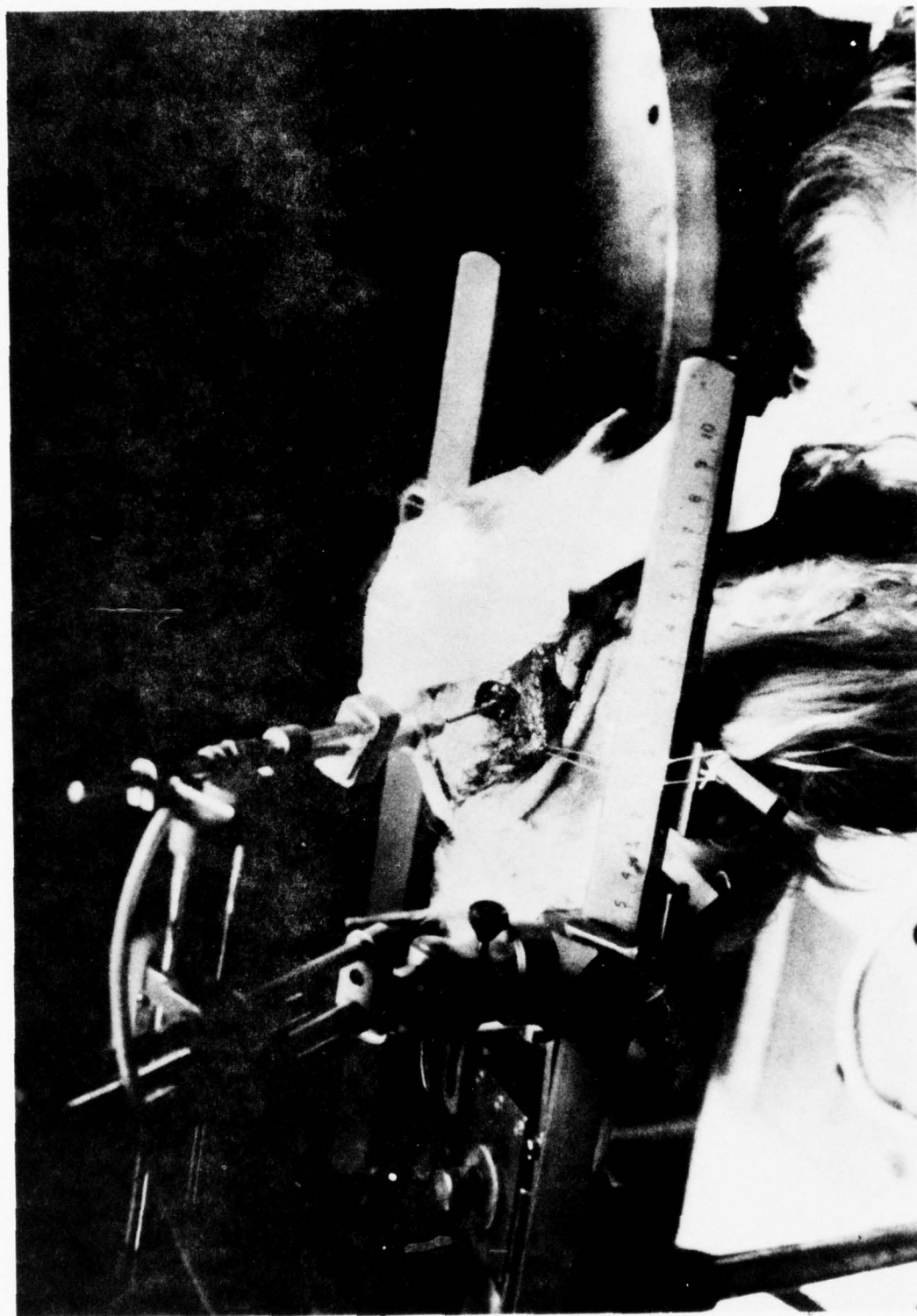


Figure 17. Probe in position for measurements of in-vivo dielectric properties of pial surface.

probe and its connecting cable could be left in the same position between measurements, the same set of termination measurements for vector error-correction could be used for a long series of in-situ tissue measurements.

During the experiment, several variables were measured simultaneously. Some of these were recorded continuously; others were recorded at discrete time increments. Time of day or time elapsed from the start of the experiment was noted along with all data recorded. The physiological parameters recorded were arterial and venous blood pressures, electrocardiogram (EKG), and blood pH, P_{O_2} , and P_{CO_2} . The blood pressures and EKG were recorded continuously on the physiograph stripchart. Values of pH, P_{O_2} , and P_{CO_2} were recorded at various times by writing down the pH/Blood Gas² Monitor readings. Continuous recording of blood parameters may be made during future experiments. Dielectric data recorded on the printer at different intervals consisted of the frequency, the amplitude and phase of the complex reflection coefficient, and the computed dielectric properties -- relative dielectric constant, conductivity, and loss tangent -- of the tissue contacted by the probe. The quantities of drugs administered to the experimental animal were also recorded.

C. Measured Results

In this subsection, the results of measurements performed during the first year of the program using the in-vivo dielectric measurement probe are presented. The principal topics addressed were the effects of the following conditions on dielectric properties at a frequency of 2450 MHz:

- changes in regional blood flow,
- different levels of physiological activity, and
- changes after death (postmortem).

Useful results were obtained from five dogs used as experimental animals. Data on live brain tissue were obtained from four animals. One dog was sacrificed before data were taken because of internal bleeding. These experiments have provided substantial preliminary data

on brain dielectric properties at 2450 MHz. Specific problem areas were also defined which are discussed later in this report.

There were four major types of measurements made according to the probe antenna location:

- Dural,
- Pial,
- Brain (shallow), and
- Brain (deep).

Dural measurements were made on the surface of the dura mater, the outermost membrane covering the brain; pial measurements were made on the pia mater, the innermost covering. The dura, a thick, tough membrane, is separated from the thin pia by cerebro-spinal fluid (CSF) in the areas where measurements were performed. The pia is very thin, elastic, and conforms to the surface of the brain. Pial measurements may thus be considered as taken on the brain's surface. Measurements were also performed with the probe at two relative depths in brain tissue. The probe tip was less than 1.3 cm below the surface for shallow brain measurements and between 1.3 and 2.5 cm for deep brain measurements. The shallow and deep measurements correspond roughly to gray and white matter, respectively.

Figure 18 presents the data obtained from an animal which was breathing into a closed bag for the period indicated by the shaded area. Measurements were made on the dura before and during the bag breathing. The procedure was carried out to increase the blood flow to the brain by increasing the CO_2 content of the inhaled gas mixture. The bag was initially filled with 10 liters of O_2 . Neglecting water vapor, the fraction of CO_2 in the bag increased linearly from 0 to about 8.8% in the 8 minutes the bag was attached to the animal's tracheal tube. During this experimental maneuver, large increases were observed in venous blood pressure and in respiratory rate and volume. The average of the values for each dielectric parameter during rebreathing into the closed bag is almost identical to that before bag breathing. It is difficult to state conclusive findings based on this preliminary experiment. However, for the particular case just described, it appears

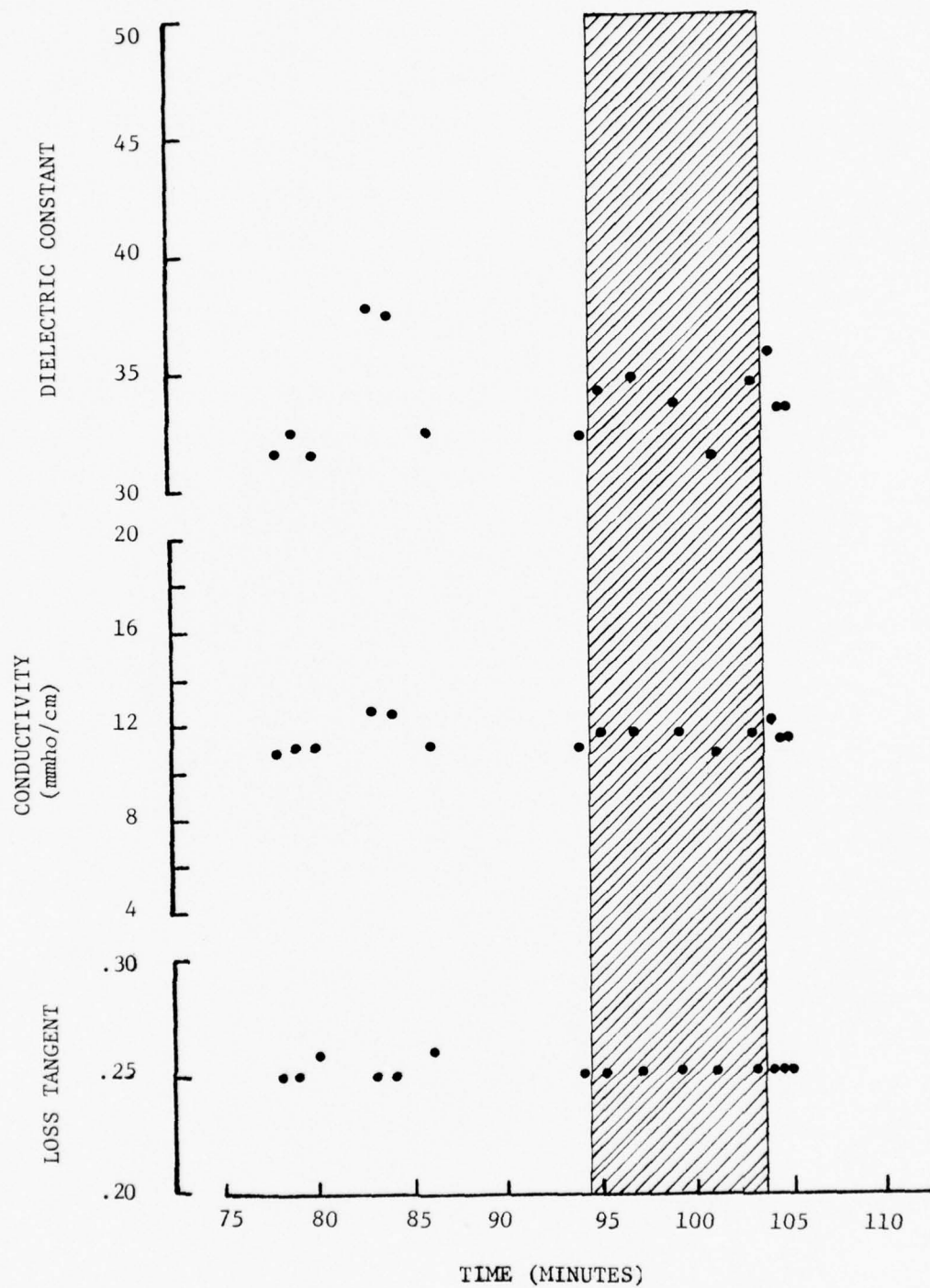


Figure 18. Measured dielectric properties of dura before and during bag breathing. The shaded area denotes bag breathing. Time is the time from the start of measurements. Brain temperature range: 35.3 to 35.5°C.

that there was no change in the extradural dielectric properties caused by the bag breathing.

The variations in values seen in this experiment for both dural and pial measurements were typical of the data obtained with a hand-held probe. In a previous experiment on dead brain tissue still in-situ, differences in computed dielectric parameters were seen to vary with the force applied to the probe during contact with the tissue. The most consistent results were obtained with firm, but not excessive, pressure. However, the tissue deteriorated more rapidly with the firm pressure applied at a single location than with light-to-moderate pressure.

To study differences in dielectric properties between live and dead brain tissue, measurements were made before, during, and after lethal injections of either pentobarbital or calcium chloride. In two animals sacrificed with pentobarbital overdoses, measurements were made with the probe in brain tissue. Figures 19 and 20 show the results from these two experiments. The data for one animal were obtained with the probe in a deep-brain position (Figure 19), and in the other animal, data were obtained with the probe in a shallow-brain position (Figure 20). Each data point for the deep-brain position is the average of three to six measurements taken within one minute. Data points for the shallow-brain position represent single measurements taken at one-minute intervals.

The time at which blood flow to the head stopped in these two experiments was taken as that time when the arterial blood pressure went to zero. At the same time, or a few seconds before, bleeding from the excised muscles of the head ceased. In both experiments, values of all three dielectric properties (dielectric constant, conductivity, loss tangent) increased after the blood flow stopped. For the shallow position, the increases in all dielectric property values began within one-minute of the cessation of blood flow. For the deep position, the increase in dielectric constant occurred between seven and ten minutes after the cessation of blood flow. Values of conductivity and loss tangent were already elevated at seven minutes. Due to technical difficulties, measurements were not made in this experiment until seven minutes following cessation of blood flow to the head, so it is possible

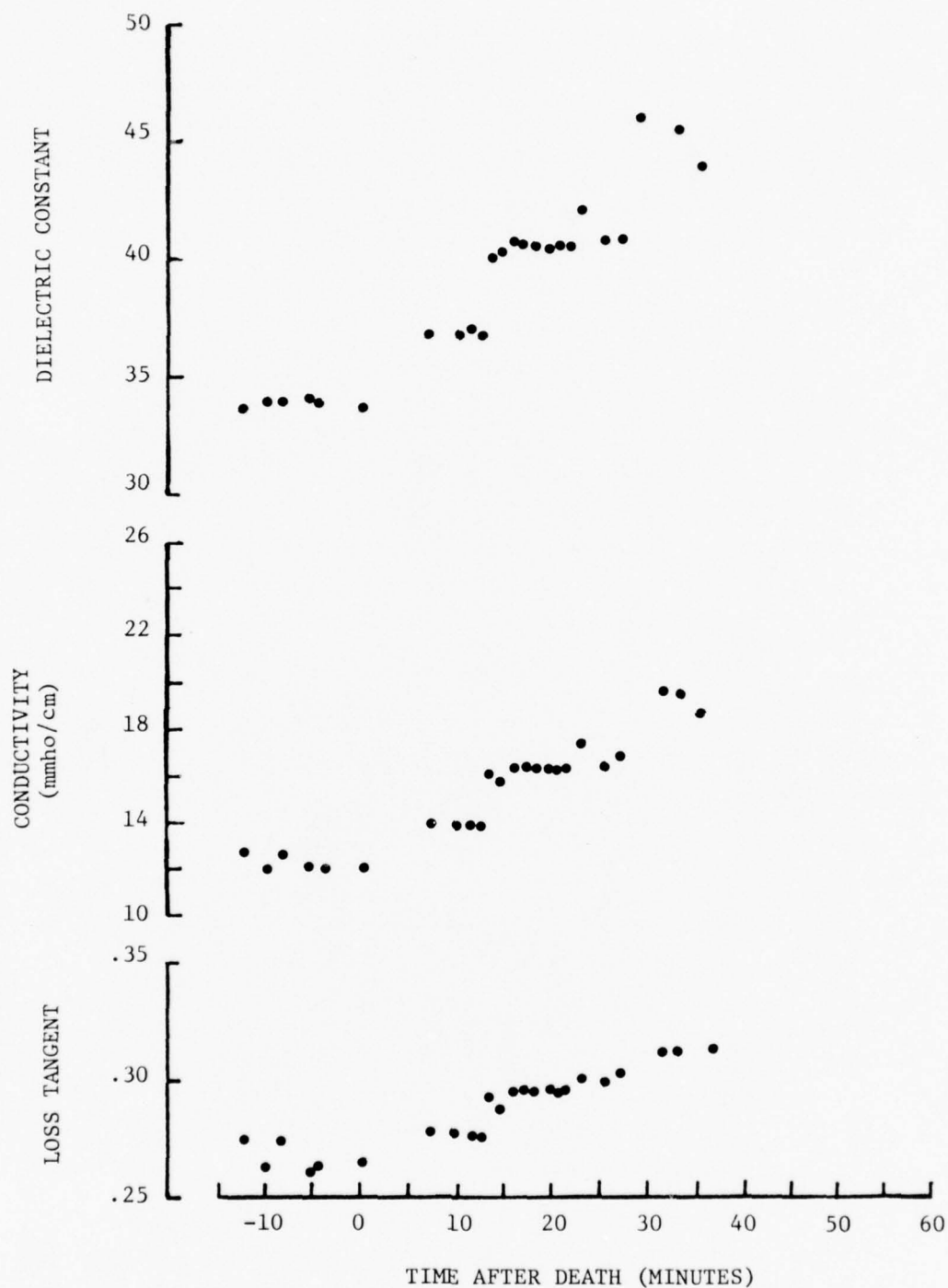


Figure 19. Measured dielectric properties of deep canine brain (white matter) as a function of time after death resulting from Pentobarbital overdose injection. Brain temperature range: 36.5 to 38.5°C.

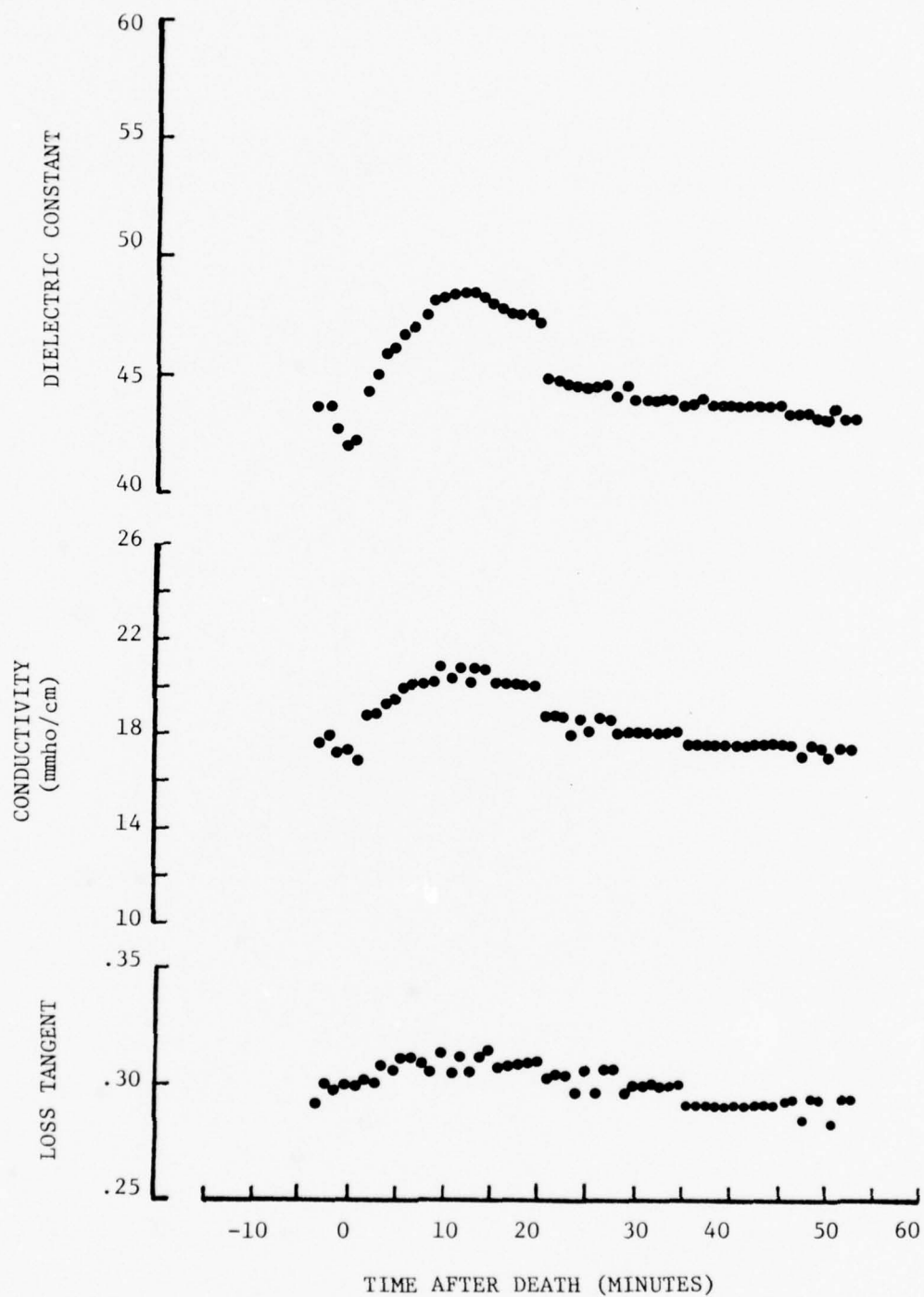


Figure 20. Measured dielectric properties of shallow canine brain (gray matter) as a function of time after death resulting from Pentobarbital overdose injection. Brain temperature range: 34.0 to 37.5°C.

that these two parameters began changing just after the blood flow stopped. The values of dielectric constant and conductivity are lower for the deep position. This can be expected if the myelin of the deeper white matter is assumed to contribute to the overall dielectric constant of the tissue at 2450 MHz. For the deep position, the values all increased monotonically until the end of the experiment at 36 minutes after the cessation of blood flow. For the shallow position, the values increased for the first seven to eight minutes, leveled off for about six minutes, and then decreased until the end of the experiment at 53 minutes after cessation of blood flow. The downward changes in these data at 20 minutes were not correlated with any physiological changes nor with adjustments in the measurement procedure.

The differences in the two time courses could be due to the different types of brain tissue measured. In other words, the type of neural tissue may determine not only the static dielectric properties, but also the changes in these properties under changes in physiological states. Alternatively, the differences in time courses may be related to blood flow changes in the tissue [15-16]. Blood flow through the gray matter (shallow) is known to be several times larger than the blood flow through white matter (deep). Thus, the effect of a cessation of blood flow to the brain would be expected to have a more rapid and larger effect on gray matter than on white matter. Changes in dielectric properties could be the direct result of the lack of blood flow or, since the metabolism of gray matter is greater than that of white matter, they could be the result of changes in metabolic processes caused by the lack of nutrients in the gray matter [16]. Because of the differences in blood flow through gray and white matter, a comparison of the changes in dielectric properties of gray and white brain matter may be a sensitive test for analyzing the effects of blood flow on dielectric properties.

Figure 21 shows the dielectric properties measured during death of an animal under different conditions than in the two experiments just described. In this experiment, the measurements were made on the pia covering the left anterior ectosylvian gyrus. Measurements were made at

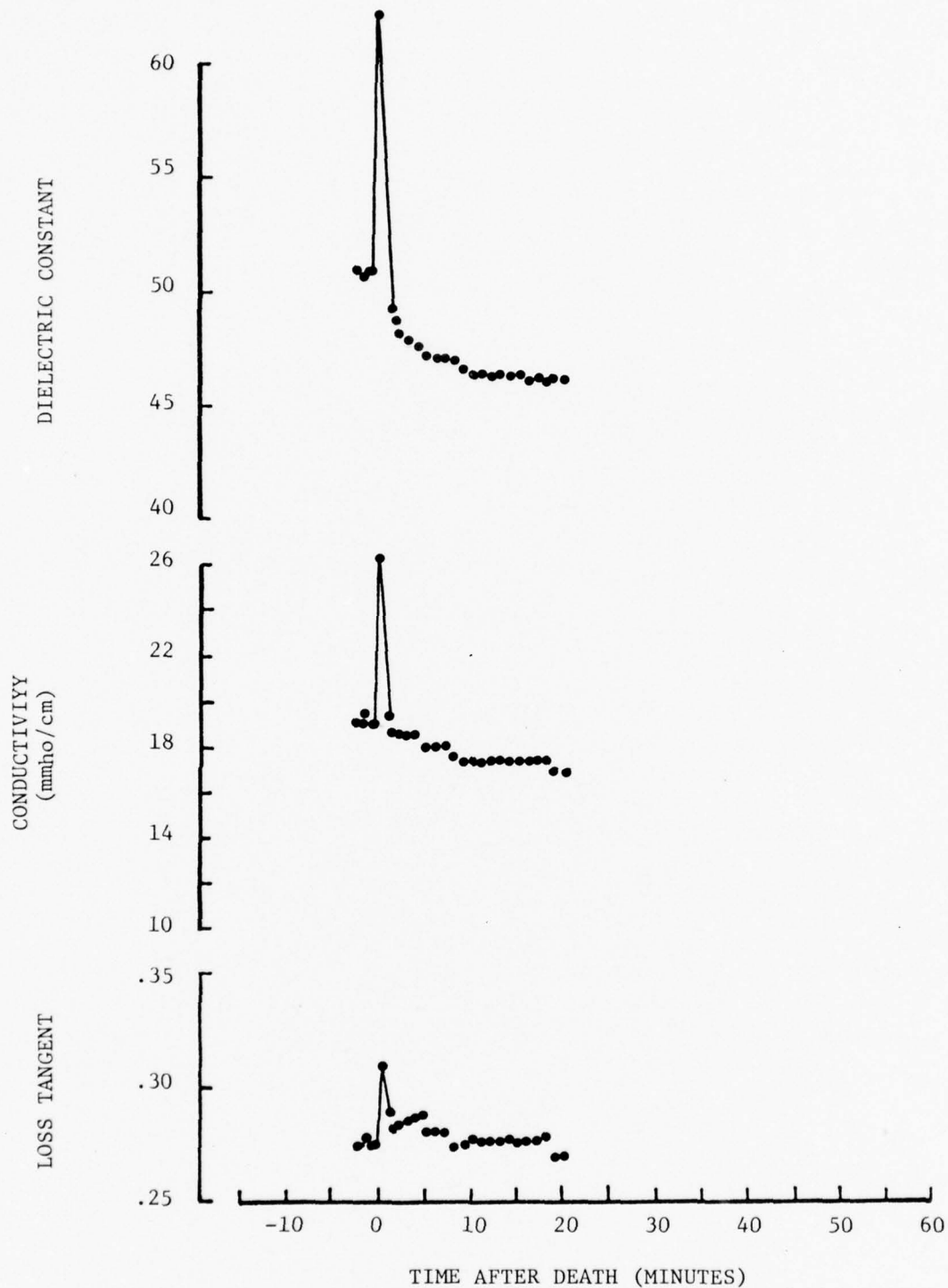


Figure 21. Measured dielectric properties of surface of brain as a function of time after death resulting from CaCl_2 injection. Brain temperature range: 35.5 to 36.0°C.

30-second intervals in this experiment. Because the dielectric properties changed slowly during most of the experiment, the data are presented at one-minute intervals except during the rapid changes near zero time. The animal was under deep anesthesia which had been induced and maintained with pentobarbital. The lethal injection was a bolus of a concentrated aqueous solution of calcium chloride (CaCl_2). The arterial blood pressure increased immediately upon this injection and then decreased to zero, all within 20 seconds after the injection. This drop of blood pressure to zero was more rapid than seen in the experiments using overdoses of pentobarbital and had a much shorter latency from the time of injection. In these respects, the results of this experiment should be more indicative of the effects of an abrupt cessation of blood flow. In Figure 21, the time zero corresponds to the time at which blood pressure reached zero, which on the time scale displayed is essentially the time of the injection. As seen in the figure, there was a rapid, very large increase in each of the three computed dielectric properties. The brain expanded during this period, corresponding to the increase in blood pressure. Subsequent to the blood pressure increase, a rapid return to values similar to those prevailing before the injection was observed, followed by a gradual decrease in all three properties.

The measurements in the experiment just described are comparable to those obtained in the shallow-brain position with pentobarbital overdose (Figure 20) since, in principle, the measurements are of gray matter at a surface and an interior location, respectively. In both cases, the values for dielectric properties first increase and then decrease, although both phases are slower for the shallow-brain case. The changes in dielectric properties at a deeper location appear to change even more slowly without a second, declining phase (Figure 19). It is thus possible that the rate of change in dielectric properties in brain tissue is a function of depth below the surface. However, it is possible that comparison among results of these experiments under conditions of differing rates of blood pressure decrease may not be valid. Comparisons among additional similar experiments or within a

single experiment are necessary to test the above hypothesis. Other influencing factors such as temperature variation, probe contact pressure, etc., should also be minimized for this purpose.

Another experimental investigation was also conducted on a dog given the lethal CaCl_2 injection. In-vivo probe measurements were made in the region of the left ectosylvian gyrus to see if dielectric property changes could be measured when different acoustic stimuli were applied to the right side of the head. The animal was prepared in the previously described manner, and the acoustic stimuli were delivered by a loud-speaker placed near the right side of the head. Two sets of measurements were performed on the dura (one anterior and one posterior) and two sets of measurements were made on the pia (one on the anterior ectosylvian gyrus (AES) and one on the posterior medial ectosylvian gyrus (PMES)). Within each set of measurements, the three following stimuli were presented:

1. no sound (control),
2. 200 Hz tone, and
3. 5 kHz tone.

The tone stimulus was always presented between two control conditions. The probe measurement was made either during or immediately following each stimulus presentation and during control conditions. If the stimuli produced a change in local neural activity, the corresponding change in local blood flow might be indicated by changes in measured dielectric properties.

The medial ectosylvian gyrus is the cortical area which receives auditory information. This primary auditory area is tonotopically organized with high frequencies represented anteriorly and low frequencies represented posteriorly. Thus, by using a high (5 kHz) or a low (200 Hz) frequency tone, it was hoped that a small region of the auditory cortex could be stimulated.

The results of these acoustic-stimulus experiments are presented in Figures 22 and 23, for the dura and pia measurements, respectively. The abscissa in each of the eight plots of dielectric properties is the average value of the control measurements performed before and after the

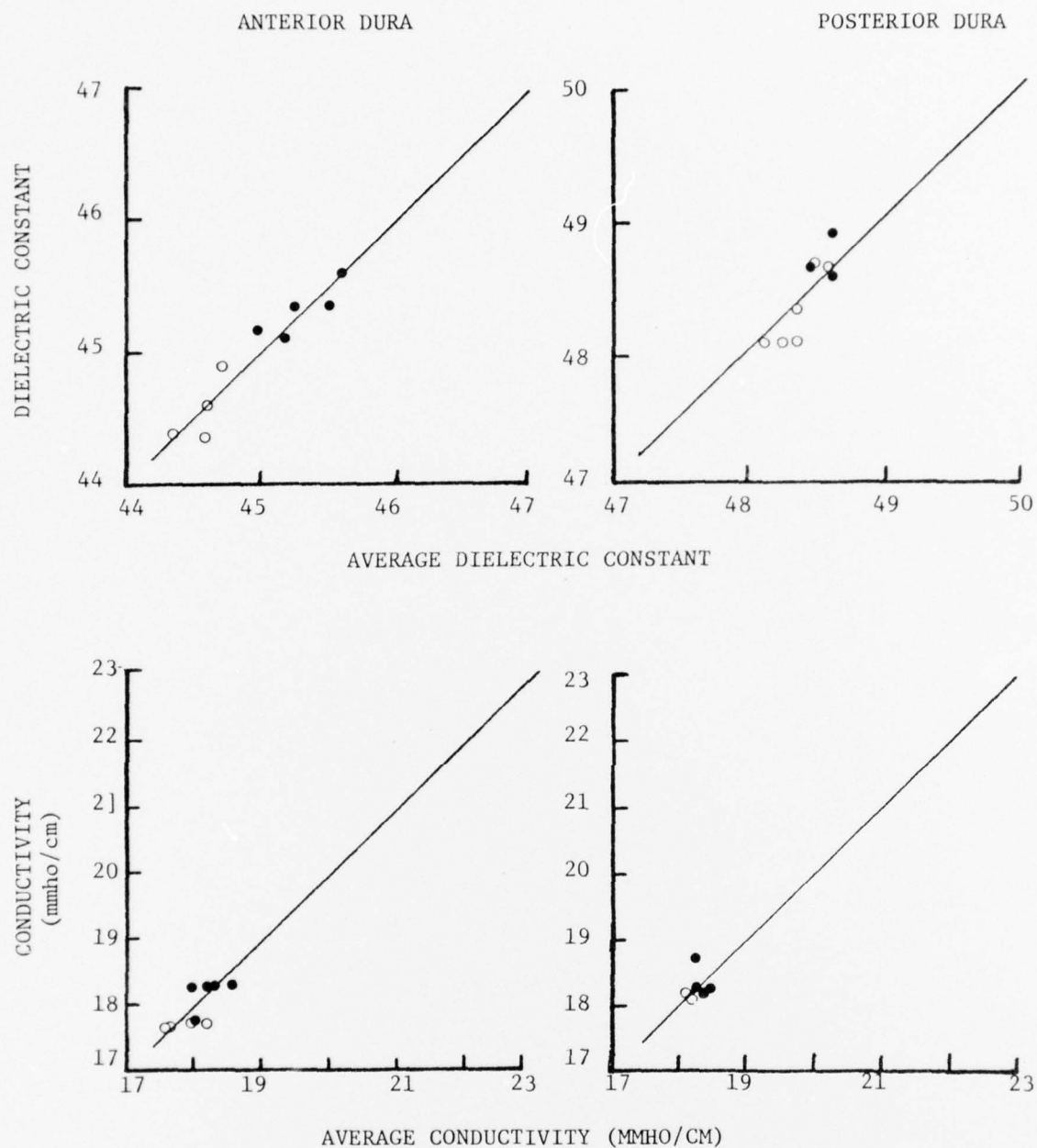


Figure 22. Results of dural measurements in acoustic stimulation experiment: solid circles are for 200 Hz; open circles, 5 kHz. Refer to text for further details.

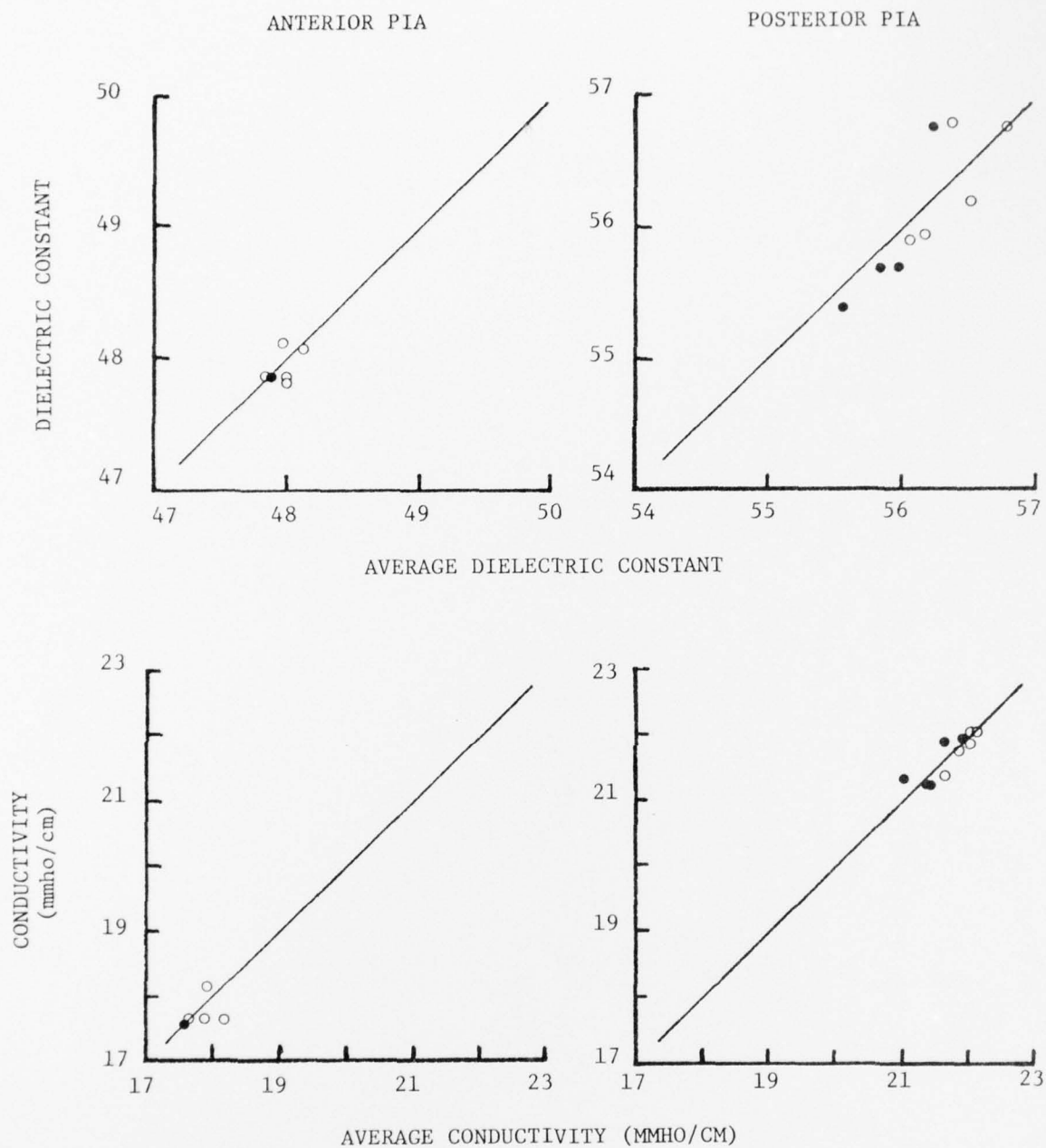


Figure 23. Results of pial measurements in acoustic stimulation experiments. Solid circles are for 200 Hz; open circles, 5 KHz. Refer to text for further details.

stimulus. The ordinate is the value measured during the stimulus. Data for both 200 Hz and 5 kHz are presented on each plot. If there were no changes in the dielectric property during the stimulus, the plot would consist of points lying on the 45 degree line drawn in the plot. It is seen in all cases that the points are scattered near this line indicating little or no effect by the acoustic stimuli on the dielectric properties measured in two locations (AES and PMES) on the pia. Two different experimental conditions may have prevented the detection of dielectric property changes in this experiment. First, the acoustic stimulus was most probably not sufficient to produce significant activity in the primary auditory area. Although the tones were relatively loud (as perceived by laboratory personnel), the solid earbars used to hold the animal's head would act to attenuate the acoustic energy received by the animal's inner ear. Second, the probe may have been placed near, but not exactly on a region of neural activity. A map formed by recording the electrical activity in the cortical regions of interest would better define placement of the probe for measuring physiological changes. An additional factor to be considered is the effect of the anesthetic on the connectivity between the auditory periphery and the cortex.

The histogram shown in Figure 24 is a summary of the measurements made on the live brain of four animals -- dogs A, B, C, and D -- as indicated by the letter designations on the individual columns. The column height represents the mean value, and the bars indicate one standard deviation above and below the mean. Standard deviations are not shown in cases where their magnitudes are so small as to be on the order of the line thickness. Data were gathered from the four probe locations noted in the figure, with most of the data being from dural and pial locations. For dog D, two different pial and two different dural positions are shown separately since the measured dielectric property values did not overlap. There are not as many data for locations beneath the surface (the shallow- and deep-brain locations) as there are for surface measurements because emphasis was placed on non-invasive (surface) measurements. For animals A and B, the probe was

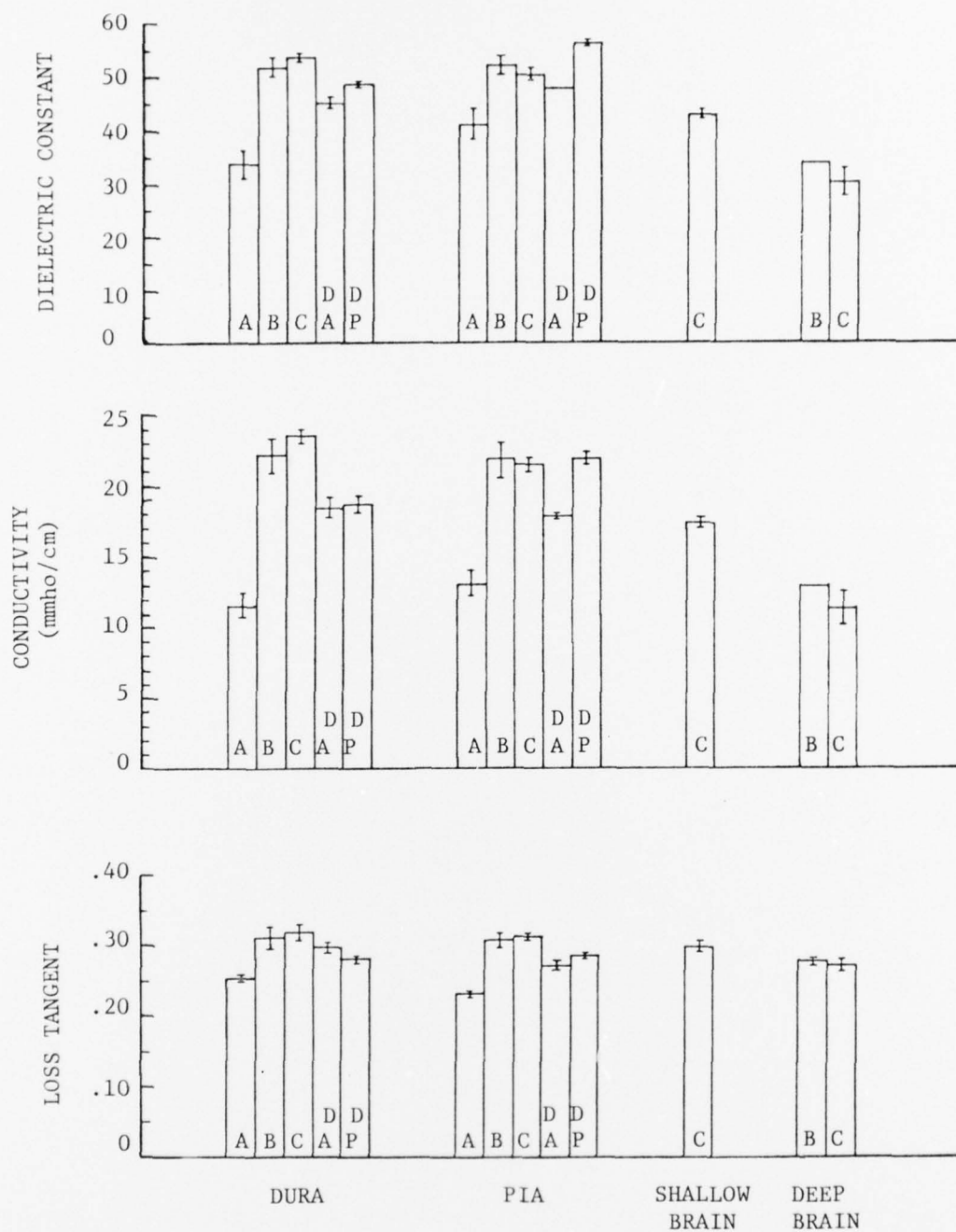


Figure 24. Summary of in-vivo brain data from four animals. Column height is the mean value. The bars indicate plus or minus one standard deviation.

held by hand, while for animals C and D, the probe was held by the electrode carrier. This difference in probe support probably accounts for the generally larger scatter (larger standard deviations) for the data from dogs A and B. Because of this scatter and the small number of measurements for animal A, the data for this animal (A) may not be representative and therefore is excluded for the remainder of this discussion. This observation emphasizes the need both for steady consistent support for the probe during measurements and for a sufficient number of measurements for each physiological and physical condition.

For the dural measurements of animals B, C, and D, the mean for dielectric constant ranges from 45.3 to 53.9; for conductivity, the mean ranges from 18.4 to 23.5 mmho/cm; for loss tangent, the mean ranges from 0.280 to 0.320. For each dielectric parameter measured on the dura, the maximum occurs for animal C and the minimum for animal D, with the values for animal B being intermediate. The differences in dielectric properties for the dura are probably due to different thicknesses of the dura itself rather than due to interanimal differences since the values for dielectric constant and loss tangent are distinctly different for two locations (anterior and posterior) in animal D. The measured properties of the dura are also influenced to a certain extent by the underlying CSF. This was demonstrated in a set of measurements in animal B in which the CSF was drained from beneath the measurement site through a small dural hole located a few millimeters away. For this condition, the measured dielectric constant was 44.0 ± 6.1 (mean \pm S.D.) reduced from 58.1 ± 1.7 measured with the CSF present. The differences in values for conductivity and loss tangent were small with overlapping sample values, and therefore are considered not significant. Based on this single experiment, it appears that the dielectric constant was changed by the presence of the CSF, while conductivity and/or loss tangent were only minimally affected. Dielectric properties of the dura would probably best be measured in a sample of dura alone, in which the sample would perhaps consist of several layers of freshly-excised dura. However, the results of such measurements would not necessarily reflect in-vivo conditions.

For the pial measurements of animals B, C, and D, the mean for dielectric constant ranges from 48.0 to 56.3; for conductivity, the mean ranges from 17.8 mmho/cm to 21.8 mmho/cm; for loss tangent, the mean ranges from 0.272 to 0.313. These pial measurements are not as patterned among animals as the dural measurements. It is noted that the values for the anterior location of animal D are smallest for each property, which means that the measured values for the posterior location of this animal were always larger than for the anterior location. Generally, for the three animals, the values for typical measurements are comparable to those obtained for the dural measurements. These values of dielectric constant and conductivity for live pia are higher than the values for dead pia, 34.0 ± 3.9 and 12.8 ± 1.7 mmho/cm, respectively, measured two hours after death in another animal. The loss tangent for the dead tissue, 0.277 ± 0.011 , was similar to the values for live tissue. The temperature of the dead brain tissue was 35.5°C at the beginning of the experiment decreasing to 31.5°C at the conclusion of the experiment.

For the shallow-brain measurements, the mean relative dielectric constant, 43.0, and the mean conductivity, 17.4 mmho/cm, are smaller than values of the respective property for both dural and pial measurements in animals B, C, and D. For the two deep-brain measurement cases, the mean values of relative dielectric constant, 33.9 and 30.6, and of conductivity, 12.8 mmho/cm and 11.3 mmho/cm, are even smaller. Thus, there seems to be a pattern of smaller dielectric constant and smaller conductivity with increasing distance below the surface of the brain. In animal C for which data is available for each measurement condition, there is a decline in each dielectric property from dura to deep-brain. This pattern may be related to the finding, as indicated above, that after the cessation of blood flow to the head, the dielectric properties at deeper locations changed more slowly than at shallow or surface locations. The relationship may well be caused by the greater blood perfusions of gray matter located near the surface of the brain. Further studies of dielectric properties with depth are needed to extend these preliminary findings. The loss tangent changed

much less with depth than did dielectric constant and conductivity. Of the three dielectric properties, the loss tangent seemed to be the least sensitive to any imposed experimental change. For all conditions, the mean loss tangent value varied from 0.272 to 0.320, an 18 percent difference, and the standard deviations were typically very small. This relative constancy in the loss tangent may be caused by the presence of enough water in the form of blood, intracellular water, and interstitial fluid to dominate this property at the microwave measurement frequency employed. The dielectric constant and conductivity seem to be parameters which were much more sensitive to position and to physiological changes.

There exist little published experimental data with which to compare the data obtained in these experiments. Using the probe technique developed in our laboratory, we have measured live rat brain in a location equivalent to the pial measurements described here [3]. At 2450 MHz, a dielectric constant of 54 and a conductivity of 20 mmho/cm were measured, both of which are in good agreement with the pial values shown in Figure 24. Measurements on homogenized brain tissue have been made 2 to 24 hours after removal from the animals [17] using a slotted line. The reported average dielectric constant was about 30 and the average conductivity ranged from 15 to 20 mmho/cm with a large amount of scatter in the data. This average dielectric constant is similar to the value for live deep brain and dead pia. The average conductivity is comparable to live pia and shallow brain, but is larger than live deep brain and dead pia. The differences between those data [17] and the data measured in our laboratory might be due to the difference between live and dead brain tissue or to the averaging effect of homogenizing the tissue.

SECTION V

CONCLUSIONS AND RECOMMENDATIONS

The research efforts performed during the first year of this two-year program have been successfully completed. The primary first-year objectives of (1) further in-vivo measurement probe development, (2) instrumentation development, (3) measurements of in-situ dielectric characteristics of living and non-living animal tissues, and (4) preliminary measurements of possible tissue dielectric property changes resulting from induced physiological changes were achieved. In this section, conclusions based on the results of the first year's efforts are first discussed, followed by recommendations for the second year efforts. These second year task recommendations include tasks which differ somewhat from those originally proposed, but which are based on the first year's results and on discussions between the Army's Technical Officer and Georgia Tech project personnel. Finally, recommendations for future efforts are presented.

A. Conclusions from Results

The infinitesimal monopole probe measurement technique was further developed and extended to permit accurate, repeatable measurements of small changes of dielectric properties in living systems with a minimal effect on those systems. Some of the problem areas which were addressed in order to meet these requirements were (1) reduction of electrical errors due to the mechanical flexing of the probe cable while positioning the probe in the measurement sample, (2) minimization of the effects of sample volume and fluid accumulation on the accuracy and repeatability of the in-vivo probe measurement technique, (3) implementation of a real-time data acquisition/data processing system, (4) inclusion of a microwave test set/connector error-correction model to correct systemic measurement errors in the real-time data processing, and (5) evaluation of the above probe/system improvements by quantitation of the probe measurement system performance via measurements of well-characterized dielectric materials. The results

displayed in Figures 13 through 15 indicate that the performance of the entire probe measurement system as depicted in Figure 7 is within the instrument errors associated with the network analyzer and within the overall system noise. However, even with the maximum accuracy obtained via vector error-correction, automatic frequency-locking, improved probe fabrication techniques, and better measurement protocol (minimization of fluid accumulation, etc.), additional work still needs to be performed to further reduce or eliminate any instrument errors, filtering of system noise, and improvement of procedures for insuring consistent probe contact.

The results of in-vivo measurements performed on dog brain tissue indicate a number of interesting findings. First, the measured dielectric properties of shallow brain tissue (gray matter) differed significantly from those of deep brain tissue (white matter). These differences could be due to actual differences in the two tissue types (greater myelination of white matter), to differences in blood flow (greater blood flow to gray matter), to metabolic differences in the two tissue types, or to a combination of these factors. Because of these measured differences, using the probe to "map" the brain as a function of depth from the pial surface to deep within the brain might possibly be a sensitive indicator for analyzing the effects of blood flow on dielectric properties. Such a "map" would also be important in modeling the head for computation of EM energy absorption because the model could then be made to more accurately represent actual tissue properties. Observations also indicated that the dielectric properties of dog brain after sacrifice always increased at the cessation of blood flow, followed by a leveling off, and then a very gradual decrease as a function of time after death. This general trend was observed for measurements in shallow brain. In deep brain, the values leveled off, but did not decrease. Measurements on the pia had trends similar to these made on shallow brain, except that the leveling off stage was absent. It also should be noted that although the trends of the changes in dielectric properties as a function of time after death are similar for the three above mentioned positions, the time course of the response

is longer the deeper the probe is located in the brain. Therefore, it is possible that the rate of change in dielectric properties of brain tissue is a function of depth below the pial surface.

The results of dielectric property measurements on the dura and on the pia during the presence or absence of a non-noxious auditory stimulus indicate little or no effect by the acoustic stimuli on the dielectric properties. These results are presented in Figures 22 and 23, for the dural and pial measurements, respectively. For the two stimulus frequencies used, 200 Hz and 5 kHz, similar results were obtained at both frequencies. However, the lack of positive results from these experiments involving auditory stimuli could have been due to two factors: (1) the stimulus level to the dog's cochlea was unknown and may not have been significant and (2) a map of the cortical region of interest based on electrical recordings of stimulus response was not used in defining the probe placement.

In summary, the data for measurements made on live brain in four dogs indicate a general decrease in the dielectric constant and conductivity as a function of depth below the surface of the brain. Further, the presence of CSF tended to influence the dielectric constant as measured through the dura, with the higher dielectric constant occurring with CSF present. Without CSF, the dielectric constant dropped to the value measured in shallow brain. In the cases of measurements on living brain tissue on the pial surface, there was a very significant difference between the dielectric constant and conductivity of living and dead tissue (equal to or greater than 30 percent, with living tissue being the higher).

The in-vivo dielectric property measurement system, procedures for data acquisition and processing, and data itself presented in this report represent an important advancement in the ability to define the dielectric characteristics of tissue in-situ and in the ability to reliably detect reasonably small changes in dielectric properties due to physiological changes. In many cases of measured dielectric results reported herein, these data represent the only available reported results of their type.

B. Recommendations Second Year Tasks

Although major advancements in the realm of dielectric measurements were accomplished during the first year of this two-year program, a number of questions of physiological significance remain. Further, the results raise additional questions that should be investigated to provide significant information to the Army in terms of EM field interaction with living tissues.

Based on discussions with the Army Contracting Officer's Technical Representative, it mutually was determined that the purposes of this research effort would be better served (1) by eliminating the originally-proposed second-year tasks associated with the development, testing, and dielectric property/absorbed power measurements with the dual probe and (2) by continuing to use the in-vivo monopole probe to record measurements of dielectric properties as a function of physiological state. Specifically, the following tasks are suggested for substitution of these originally proposed for the second-year effort:

- (1) Development of techniques to further reduce any remaining systemic errors. These efforts would include filtering of residual system noise and development of a method for maintaining constant, uniform probe contact pressure during in-situ measurements.
- (2) Develop a method for time-locking the data sampling to the respiratory cycle, if needed, to further circumvent changes in probe contact.
- (3) Implement a system for rapid mass storage of data.
- (4) Perform antemortem/postmortem probe dielectric measurements of the pial surface under pentobarbital anesthesia and CaCl_2 sacrifice.
- (5) Quantitatively characterize the effects of blood flow on dielectric properties of tissue at a constant temperature in a simple model. Dielectric measurements of muscle tissue would be performed where the blood supply has been isolated and the blood flow can be independently regulated and measured.
- (6) Determine the effects of auditory stimulation on the dielectric properties of auditory cortex at the pial surface due to local changes in cerebral blood flow. This will be accomplished by performing in-vivo dielectric measurements of the cortex under different stimulus parameters. Stimulus

variations would include intensity, duration, and repetition rate. Further, it is important that any measured dielectric property changes be correlated with measured changes in electrical potentials.

C. Recommended Future Efforts

During the discussions between the Army Contracting Officer's Technical Representative and project personnel from Georgia Tech, additional tasks were identified which would require additional resources and time to accomplish. Because of the detailed experimental nature of these investigations, it is recommended that resources be allocated to perform additional tasks in third- and fourth-year efforts. Specifically, the following additional tasks are recommended:

- (1) Perform experiments under hypercapnic and anoxic conditions to determine effects of regional cerebral blood flow on in-vivo dielectric properties (under halothane anesthesia).
- (2) Repeat the key auditory stimulation studies performed during the second year of the current program using halothane anesthesia rather than chloralose or pentobarbital.
- (3) Perform detailed measurements of renal dielectric properties as a function of renal blood flow, changes in the juxtaglomerular apparatus, and glomerular filtration rate changes.
- (4) Perform additional efforts toward development of a truly needle probe to permit "mapping" of tissue dielectric characteristics at various locations within the tissue or organ.
- (5) Characterize brain tissue as a function of depth beneath the pial surface by performing dielectric measurements using a smaller-diameter (0.047 inch) in-vivo probe.
- (6) Perform studies of the effects of visual stimulation on in-vivo dielectric properties of brain tissue (on pia) in the same manner as the auditory stimulation studies. Include independent studies of renal blood flow and somatosensory evoked potentials to correlate with dielectric studies.
- (7) Perform measurements of stimulus response through the intact dura using a larger diameter probe (0.141- or 0.250-inch) and repeat hypercapnic/anoxic and antemortem/postmortem studies.

SECTION VI

REFERENCES

1. H.A. Ecker, E.C. Burdette, F.L. Cain, and J. Seals, "In-Vivo Determination of Energy Absorption in Biological Tissue," Annual Technical Report, Project A-1755, U.S. Army Research Office Grant No. DAAG29-75-G-0182, July 1976.
2. F.L. Cain, E.C. Burdette, and J. Seals, "In-Vivo Determination of Energy Absorption in Biological Tissue," Annual Technical Report, Project A-1755, U.S. Army Research Office Grant No. DAAG29-75-G-0182, July 1977.
3. E.C. Burdette, F.L. Cain, and J. Seals, "In-Vivo Determination of Energy Absorption in Biological Tissue," Final Technical Report, Project A-1755, U.S. Army Research Office Grant No. DAAG29-75-G-0182, January 1979.
4. A.R. Von Hippel, DIELECTRIC MATERIALS AND APPLICATIONS, M.I.T. Press, 1954, pp. 36-40, 301-425.
5. W.S. Spector, HANDBOOK OF BIOLOGICAL DATA, W.B. Saunders Company, p. 291.
6. G.A. Deschamps, "Impedance of an Antenna in a Conducting Medium," IRE Transactions on Antennas and Propagation, September 1962, pp. 648-650.
7. E.C. Burdette, F.L. Cain, and J. Seals, "In-Vivo Probe Measurement Technique for Determining Dielectric Properties at VHF Through Microwave Frequencies," submitted for publication in IEEE Transactions on Microwave Theory and Techniques.
8. R.L. Magin, and C.P. Burns, "Determination of Biological Tissue Dielectric Constant and Resistivity from In-Vivo Impedance Measurements," Region Three Conference of the IEEE, April 1972.
9. C.T. Tai, "Characteristics of Linear Antenna Elements," ANTENNA ENGINEERING HANDBOOK, Chapter 3, H. Jasik, Editor, McGraw-Hill, 1961, p. 2.
10. J.H. Richmond, "A Reaction Theorem and Its Application to Antenna Impedance Calculations," IRE Transactions on Antennas and Propagation, November 1961, pp. 515-520.
11. Semi-Automated Measurements Using the 8410B Microwave Network Analyzer and the 9825A Desk-Top Counter, Hewlett-Packard Application Note 221, March 1977.
12. F. Buckley, and A.A. Maryott, "Tables of Dielectric Dispersion Data for Pure Liquids and Dilute Solutions," National Bureau of Standards Circular 589, November 1958.

13. H. F. Cook, "A Comparison of the Dielectric Behavior of Pure Water and Human Blood at Microwave Frequencies," British Journal of Applied Physics, Vol. 3, August 1952, pp. 249-255.
14. J.B. Hasted, Water: A Comprehensive Treatise (The Physics of Physical Chemistry of Water), Ed., F. Franks, Plenum Press, New York - London, Volume 2, 1972, pp. 255-305.
15. O. Sakurada, C. Kennedy, J. Jehle, J.D. Brown, G.L. Corbin, and L. Sokoloff, "Measurement of local cerebral blood flow with iodo ^{14}C antipyrine," American Journal of Physiology 234, 1978, pp. H59-H66.
16. W.A. Pulsinelli, and T.E. Duffy, "Local Cerebral Glucose Metabolism During Controlled Hypoxemia in Rats," Science 204, 1979, pp. 626-629.
17. J.C. Lin, "Microwave Properties of Fresh Mammalian Brain Tissues at Body Temperatures," IEEE Transactions on Biomedical Engineering, BME-22, 1975, pp. 74-76.